Combined Intramyocardial Delivery of Human Pericytes and Cardiac Stem Cells Additively Improves the Healing of Mouse Infarcted Hearts Through Stimulation of Vascular and Muscular Repair

Elisa Avolio, Marco Meloni, Helen L. Spencer, Federica Riu, Rajesh Katare, Giuseppe Mangialardi, Atsuhiko Oikawa, Iker Rodriguez-Arabaolaza, Zexu Dang, Kathryn Mitchell, Carlotta Reni, Valeria V. Alvino, Jonathan Rowlinson, Ugolini Livi, Daniela Cesselli, Gianni Angelini, Costanza Emanueli, Antonio P. Beltrami, Paolo Madeddu

Rationale: **Optimization of cell therapy for cardiac repair may require the association of different cell populations with complementary activities.**

Objective: **Compare the reparative potential of saphenous vein–derived pericytes (SVPs) with that of cardiac stem cells (CSCs) in a model of myocardial infarction, and investigate whether combined cell transplantation provides further improvements.**

Methods and Results: **SVPs and CSCs were isolated from vein leftovers of coronary artery bypass graft surgery and discarded atrial specimens of transplanted hearts, respectively. Single or dual cell therapy (300 000 cells of each type per heart) was tested in infarcted SCID (severe combined immunodeficiency)-Beige mice. SVPs and CSCs alone improved cardiac contractility as assessed by echocardiography at 14 days post myocardial infarction. The effect was maintained, although attenuated at 42 days. At histological level, SVPs and CSCs similarly inhibited infarct size and interstitial fibrosis, SVPs were superior in inducing angiogenesis and CSCs in promoting cardiomyocyte proliferation and recruitment of endogenous stem cells. The combination of cells additively reduced the infarct size and promoted vascular proliferation and arteriogenesis, but did not surpass single therapies with regard to contractility indexes. SVPs and CSCs secrete similar amounts of hepatocyte growth factor, vascular endothelial growth factor, fibroblast growth factor, stem cell factor, and stromal cell–derived factor-1, whereas SVPs release higher quantities of angiopoietins and microRNA-132. Coculture of the 2 cell populations results in competitive as well as enhancing paracrine activities. In particular, the release of stromal cell–derived factor-1 was synergistically augmented along with downregulation of stromal cell–derived factor-1–degrading enzyme dipeptidyl peptidase 4.**

Conclusions: **Combinatory therapy with SVPs and CSCs may complementarily help the repair of infarcted hearts. (*Circ Res*. 2015;116:e81-e94. DOI: 10.1161/CIRCRESAHA.115.306146.)**

Key Words: acute inferior myocardial infarction ■ cardiac remodeling, ventricular ■ cell- and tissue-based therapy ■ cell transplantation ■ pericytes ■ stem cells

Millions of cardiac cells are lost immediately after an acute myocardial infarction (MI), thus critically endangering the heart's functional performance. Although a spectrum of spontaneous reparative reactions is activated to restore perfusion and contractility, these attempts are usually insufficient and also associated with adverse remodeling responses, which eventually lead to ventricular dysfunction and failure.

The underlying concept of cell therapy for cardiac repair is to provide the infarcted heart with exogenous supplements of regenerative elements to boost reparative vascularization and cardiomyogenesis. Transplantation of autologous stem cells currently represents the most popular and safe supply-side option. However, owing to their limited plasticity, single adult stem cell populations may not provide the desired multipurpose

Original received January 29, 2015; revision received March 13, 2015; accepted March 23, 2015. In February 2015, the average time from submission to first decision for all original research papers submitted to *Circulation Research* was 13.9 days.

From the Experimental Cardiovascular Medicine (E.A., H.L.S., F.R., R.K., G.M., A.O., I.R.-A., Z.D., K.M., C.R., V.V.A., J.R., P.M.) and Vascular Pathology and Regeneration (M.M., C.E.), School of Clinical Sciences, University of Bristol, Bristol, United Kingdom; Institute of Cardiovascular and Medical Sciences (M.M.), University of Glasgow, Glasgow, United Kingdom; Department of Physiology, University of Otago, Dunedin, New Zealand (R.K.); Department of Medical and Biological Sciences (D.C., A.P.B.) and Department of Experimental Medical and Clinical Sciences (U.L.), University of Udine, Udine, Italy; and Cardiac Surgery, Bristol Heart Institute, School of Clinical Sciences, University of Bristol, Bristol, United Kingdom (G.A.).

The online-only Data Supplement is available with this article at http://circres.ahajournals.org/lookup/suppl/doi:10.1161/CIRCRESAHA.115.306146/-/DC1.

Correspondence to Paolo Madeddu, MD, Experimental Cardiovascular Medicine, Bristol Heart Institute, University of Bristol, Upper Maudlin Rd, Bristol BS2 8HW, United Kingdom. E-mail Paolo.Madeddu@bristol.ac.uk

Nonstandard Abbreviations and Acronyms

ANG1/2	angiopoietin1/2
CSCs	cardiac stem cells
DPP-4	dipeptidyl peptidase-4
EdU	5-ethynyl-2′-deoxyuridine
LV	left ventricular
MI	myocardial infarction
MSC	mesenchymal stromal cell
miR-132	microRNA-132
SDF-1α	stromal cell–derived factor 1α
SVPs	saphenous vein–derived pericyte progenitors

solution. Apart from a recent study reporting the benefit of associative treatment with human mesenchymal stromal cells (MSCs) and human c-Kit$^+$ cardiac stem cells (CSCs) in an immunosuppressed swine model of MI,[1] combinatory cell therapy has received little attention. In particular, to the best of our knowledge, no previous study has investigated the advantage of dual therapy with cardiac and vascular stem/progenitor cells for harmonized repair of the infarcted heart.

CSCs have already been tested in first-in-human studies,[2–5] in spite of some persistent uncertainty around their capacity to differentiate into mature cardiomyocytes and vascular cells in vivo.[6–8] In the SCIPIO (Cardiac Stem Cell Infusion in Patients With Ischemic CardiOmyopathy) trial, cardiac cells were isolated from the right atrial appendage of patients undergoing coronary artery bypass graft surgery, expanded and immunoselected to obtain c-Kit$^+$ CSCs.[2] In the CADUCEUS (CArdiosphere-Derived aUtologous stem CElls to reverse ventricULar dysfunction) study, cells were derived from percutaneous endomyocardial biopsy specimens and grown in primary culture where they develop multicellular clusters known as cardiospheres.[4,5] Cardiosphere-derived cells contain a mixture of stromal and mesenchymal cells, including c-Kit$^+$ CSCs. Both studies did not raise safety concerns and showed encouraging results in terms of cardiac function improvement and scar size reduction.[2–5] However, definitive clinical exploitation of c-Kit$^+$ CSCs requires further verification and certification.[9,10]

Vascular pericytes are gaining momentum as a potential vasculogenic approach, but they still stand at the preclinical stage of experimentation.[11–13] Noteworthy, pericytes are abundant in the heart, play important roles in vascular growth and stabilization, and act as an interface between the coronary circulation and the cardiomyocyte compartment.[14] However, harvesting pericytes from a patient's heart entails an invasive procedure. To circumvent this problem, we have been focusing on discarded saphenous vein remnants from coronary artery bypass graft surgery as a source of vascular pericytes. By recycling leftover products, we have developed a sustainable cell therapy approach which was proven to help vascular and muscular repair in models of peripheral and myocardial ischemia.[12,15] Transplanted pericytes directly incorporate into the recipient vasculature and also stimulate reparative angiogenesis in a paracrine manner. Interestingly, among the angiocrine factors secreted by pericytes, the microRNA-132 (miR-132) emerged as a multifunctional mechanism to promote angiogenesis and inhibit interstitial fibrosis. Moreover, pericytes indirectly induce endogenous cardiomyogenesis, by stimulating cardiomyocyte proliferation and attracting resident CSCs.[12]

This investigation aims to determine whether combined transplantation of saphenous vein–derived pericyte progenitors (SVPs) and CSCs sourced from discarded surgical tissue promotes the healing of mouse infarcted hearts better than single cell therapy. We show for the first time that the advantage of dual cell therapy derives from complementary actions on the recipient infarcted heart as well as transcriptional and post-transcriptional interactions between the donor populations.

Methods

Expanded Methods are provided in the Online Data Supplement.

Human CSCs were isolated from discarded atrial specimens of hearts donated for transplantation.[16] Human SVPs were immunosorted from vein leftovers of coronary artery bypass graft surgery patients.[12,15] The main characteristics of donors are reported in Online Table. Cells were compared with regard to their antigenic phenotype and differentiation ability toward cardiovascular lineages. Interactions between cocultured SVPs and CSCs and paracrine effects on murine CSCs, cardiomyocytes, and endothelial cells were investigated in vitro.

In in vivo studies, severe combined immunodeficiency (SCID)-Beige mice were intramyocardially injected with vehicle, SVPs, CSCs, or SVPs+CSCs (n=5–7 mice per group, total dosage of 300 000 cells for each cell type), at the occasion of operative induction of MI. Cells were given at 3 different sites along the infarct border zone (final volume of 5 μL at each site) via micromanipulator-guided injection.[12] Cell dosage was decided on the basis of previous in vivo titration studies and consideration of the cell density/injection volume that can be accommodated in the mouse ventricular wall without producing myocardial damage.[12,17,18] Recovery of cardiac function was compared by echocardiography at 14 and 42 days from MI and cell therapy. Sham-operated mice (n=6) were included as control. Additional studies were conducted to investigate the effect of cell therapy on proliferation (n=6 mice per each MI group and n=3 sham operated mice). To this purpose, mice were administered with intraperitoneal injections of 5-ethynyl-2′-deoxyuridine (EdU) every 2 days.[19]

Results

Antigenic Phenotype and Differentiation Capacity

We first compared the antigenic profile of human SVPs and CSCs. As shown in Figure 1A, immunofluorescence analysis indicates that both cell types consistently express the pericyte markers NG2 (neural/glial antigen 2) and PDGF-Rβ (platelet-derived growth factor receptor-beta) and are partly positive for the stemness marker SOX-2 ((sex determining region Y)-box 2). However, c-Kit, NANOG (homeobox NANOG), and OCT-4 (octamer-binding transcription factor 4) were uniquely expressed by CSCs (with c-Kit expressed by 85.6±2.6% of CSCs, as assessed by flow cytometry (Online Figure IA). As shown in Figure 1B, flow-cytometry analysis indicates that both cell types abundantly express the mesenchymal markers CD105, CD44, and CD90, while being negative for endothelial (CD31) and hematopoietic (CD45) antigens and for the surface glycoprotein CD34, which is typical of early hematopoietic and endothelial progenitor cells[20] as well as of vascular wall-resident stem cells.[21–24] It should be emphasized that SVPs derive from immunosorted CD34$^+$ cells, but become CD34$^-$ during culture expansion.[15]

We next investigated the differentiation capacity toward cardiovascular lineages. By immunofluorescence microscopy,

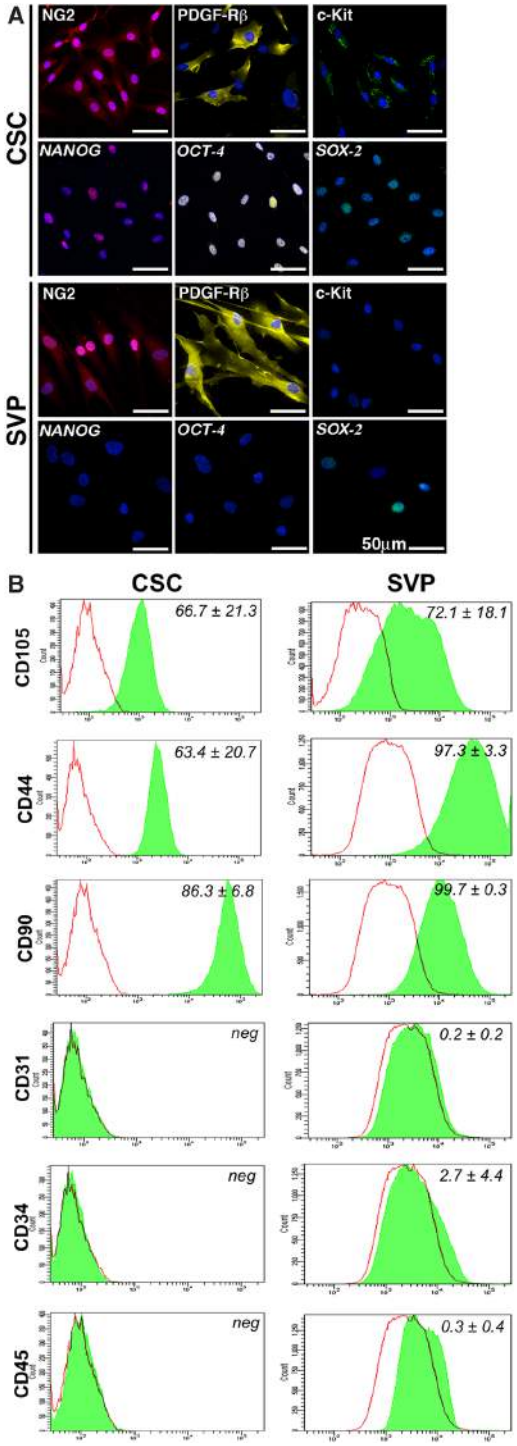

Figure 1. Cell characterization. **A**, Epifluorescence microscopy analysis of cardiac stem cells (CSCs) and saphenous vein–derived pericytes (SVPs) for the expression of the pericyte markers NG2 (neural/glial antigen 2) and PDGF-Rβ (platelet-derived growth factor receptor-beta), the stem cell factor receptor c-Kit and the stemness markers NANOG (homeobox NANOG), OCT-4 (octamer-binding transcription factor 4) and SOX-2 ((sex determining region Y)-box 2). Nuclei are shown by the blue fluorescence of 4′,6-diamidino-2-phenylindole. Scale bar, 50 μm. **B**, Flow-cytometry analysis of cultured CSCs and SVPs. Isotype control IgG staining profiles are shown by the red border line histograms, whereas specific antibody staining profiles are shown by full green histograms. For each cell type, histograms representative of 1 of the 7 cell lines analyzed have been shown. The percentages of markers expression relative to all the cell lines (n=7 CSCs; n=7 SVPs) are reported on the graphs as mean±SEM.

we confirmed the ability of CSCs to acquire markers of endothelial (CD31), smooth muscle (α-smooth muscle actin), and cardiomyocyte lineages (myosin heavy chain), when cultured for 2 to 3 weeks in specific inductive media (Online Figure IB).[16] After in vitro exposure to 2 distinct media that support CSC differentiation into cardiomyocytes,[16,25] SVPs showed an upregulation of the constitutively expressed connexin-43 and became positive for α-sarcomeric actin (Online Figure IIA and IIB). In addition, both differentiation protocols induced Tbx5 and connexin-43 gene expression at mRNA level, as assessed by quantitative polymerase chain reaction analysis (Online Figure IIC and IID). However, SVPs failed to express other cardiomyocyte markers, such as cardiac troponin T (cTNNI3), myosin heavy chain (Myh7), Islet1, NKX2.5, and RyR2. Under induction of vascular differentiation, SVPs do not acquire vascular smooth muscle cell and endothelial cell markers (α-smooth muscle actin and CD31, respectively) as assessed by immunofluorescence microscopy (data not shown). This is consistent with our previous report showing maintenance of native pericyte characteristics in vitro as well as in vivo after implantation in the mouse infarcted myocardium.[12,15] Phenotypic and differentiative differences between CSCs and SVPs provide further rationale for direct face-to-face confrontation of the 2 cell populations in in vivo studies.

Effect of Single and Dual Cell Therapy in a Model of MI

We next investigated the reparative capacity of single (300 000 cells per heart) or combined cell therapy (300 000 CSCs+300 000 SVPs per heart) in immunodeficient SCID/Beige mice that were subjected to acute MI by coronary artery ligature. Two follow-up studies were conducted to assess early (14 days) and late (42 days) outcomes (Figure 2).

Functional and Hemodynamic Outcomes

Echocardiography and intraventricular pressure data indicate that transplantation of single or combined cell populations enhances the spontaneous recovery from MI, with a remarkable improvement in ventricular function compared with vehicle at 14 days post MI (Figure 3A and 3B). In particular, we found that SVPs improved a spectrum of contractility indexes, such as stroke volume, cardiac output, left ventricular (LV) ejection fraction, fractional shortening, and the rate of LV pressure rise (dP/dt max), when compared with vehicle-receiving mice. CSCs significantly ameliorated LVEF. Comparing the 2 cell populations, SVPs outperformed CSCs with regard to fractional shortening. Furthermore, the combined cell transplantation did not show additive functional and hemodynamic improvements as compared with the single cell therapies. The beneficial effect of cell therapy persisted at the 42-day follow-up assessment (Online Figure III).

Engraftment and In Vivo Differentiation of Transplanted Cells

The low survival rate of transplanted cells remains a major limitation of cell therapy.[26–28] Moreover, it is not known whether donor cells resist differently within the ischemic myocardium when injected alone or in combination. Therefore, we verified the presence of human cells in the mouse heart using 2 different techniques: (1) by prelabeling SVPs and CSCs before

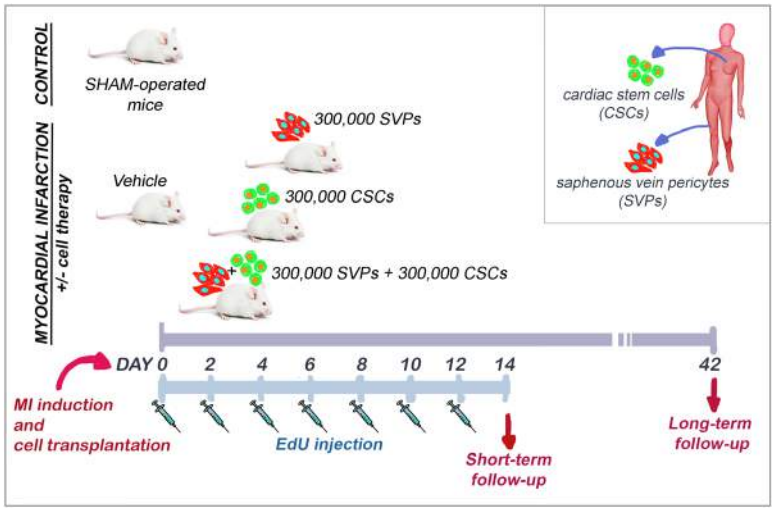

Figure 2. Schematic drawing of the experimental plan for the in vivo studies performed in a mouse model of myocardial infarction (MI). SCID (severe combined immunodeficiency)/Beige-immunodeficient mice were intramyocardially injected with saphenous vein–derived pericytes (SVPs; 300 000 cells per heart), cardiac stem cells (CSCs; 300 000 cells per heart), SVPs+CSCs (300 000 cells of each type per heart) or vehicle at the occasion of MI induction, and euthanized 14 or 42 days thereafter. Sham-operated mice were included as control. For the short-term follow-up study, a group of animals were injected with 5-ethynyl-2′-deoxyuridine (EdU) every 2 days, for proliferation studies.

transplantation with the long-term cell trackers VyBrant DiL and DiO (from Life Technologies), respectively and (2) by fluorescent immunostaining with an antibody that selectively recognizes human nuclear antigens. We found that, at 14 days post injection, clusters of SVPs were present in all the sections analyzed (5–10 for each heart cut at different levels along the infarcted LV) both within the infarct zone and in the region bordering the infarction (Online Figure IVA, IVC, IVD). This result is consistent with our previous findings documenting the peculiar resilience of SVPs to ischemic stress.[12,29] Clusters of human CSCs could be also detected in the recipient heart, although they were not present in all the samples and were less abundant than SVPs (Online Figure IVB, IVE, and IVF). In hearts receiving combined cell therapy (in which cells were labeled with DiL and DiO), we did not observe increased engraftment or spatial connections between SVPs and CSCs.

Importantly, neither SVPs nor CSCs were positive for the endothelial murine marker isolectin-B4, suggesting the lack

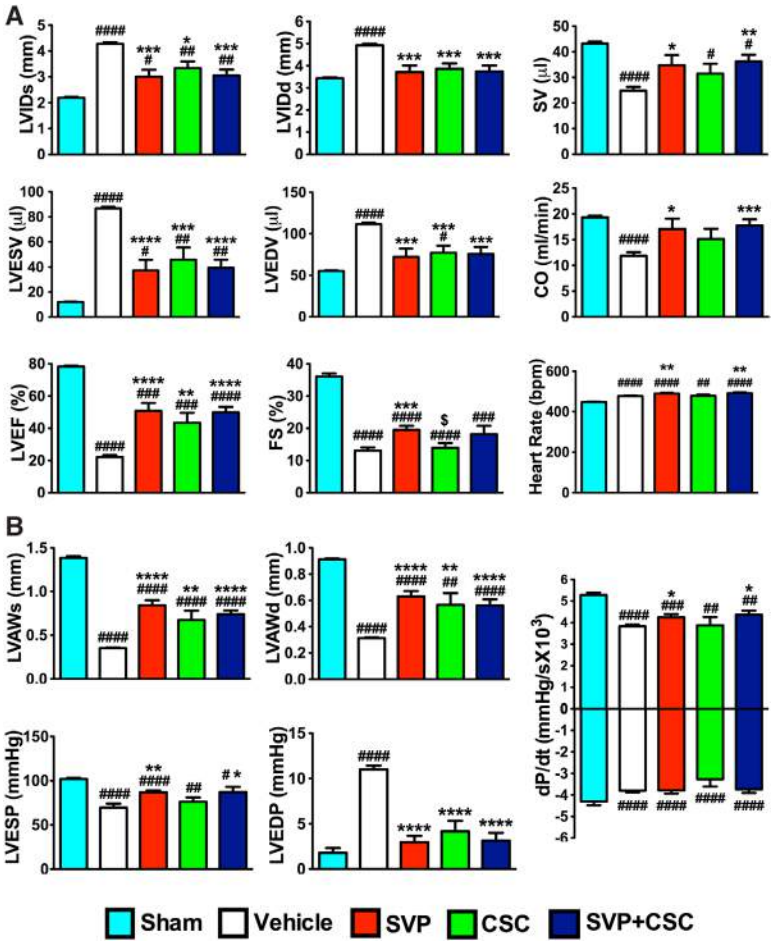

Figure 3. Effect of single or combined cell therapy on echocardiographic and hemodynamic parameters 14 days after myocardial infarction (MI). Data are presented as mean±SEM (n=6–7 mice per group). $^{\#}P<0.05$, $^{\#\#}P<0.01$, $^{\#\#\#}P<0.001$, and $^{\#\#\#\#}P<0.0001$ vs Sham; $^{*}P<0.05$, $^{**}P<0.01$, $^{***}P<0.001$, and $^{****}P<0.0001$ vs vehicle; $^{\$}P<0.05$ vs saphenous vein–derived Pericytes (SVP). CO indicates cardiac output; FS, fractional shortening; LVAWd, left ventricular anterior wall at diastole; LVAWs, left ventricular anterior wall at systole; LVEDP, left ventricular end-diastolic pressure; LVEDV, left ventricular end-diastolic volume; LVEF, left ventricular ejection fraction; LVESP, left ventricular end-systolic pressure; LVESV, left ventricular end-systolic volume; LVIDd, left ventricular internal diameter at diastole; LVIDs, left ventricular internal diameter at systole; and SV, stroke volume.

of an in vivo differentiation into endothelial cells (Online Figure IVC and IVE). In addition, rare isolated SVPs express the endothelial human antigen CD34 (Online Figure IVD) and a few human CSCs, but not SVPs, express the cardiomyocyte marker α-sarcomeric actin, suggesting an in situ differentiation of the former cells into cardiomyocyte-precursor cells (Online Figure IVF).

At 42 days post injection, no CSCs or SVPs could be detected in the recipient hearts. In all the analyses performed, we included a human myocardial sample as a positive control to verify the labeling efficiency of the antihuman nuclear antibody (labeling efficiency, 96%; Online Figure V). Moreover, we verified that the cell trackers are taken up by >90% of cells (data not shown). Finally, we performed a spectral dye separation to validate the specificity of the antihuman nuclei antibody immunofluorescence signal (Online Figure VI).

Infarct Size, Interstitial Fibrosis, and Ventricular/Cardiomyocyte Remodeling

We next assessed the effect of cell therapy on infarct size and interstitial fibrosis in the spared myocardium. Results indicate a trend toward infarct reduction by single cell therapy as compared with vehicle ($P>0.2$). However, only the group given dual cell therapy manifested a significant decrease in the volume of LV occupied by the scar ($P<0.05$ versus vehicle at 14 days post injection; Figure 4A). At 42 days, linear measurement of the scar confirmed the beneficial effect of dual cell therapy, although the difference versus single cell therapy did not reach statistical significance (Online Figure VII). In addition, single and dual cell therapies were equivalent in attenuating interstitial fibrosis ($P<0.0001$; Figure 4B).

In order to evaluate the effect of cell therapy on postinfarct remodeling, we measured the weight of LV after dissecting it from the other parts of the heart (Online Figure VIII). As shown in Figure 4C, LV weight was increased in the MI group given vehicle ($P<0.05$ versus sham operated), with this effect being attenuated by cell therapy. After an acute MI, myocyte volume is increased as an attempt to compensate the loss of myocardial mass. Therefore, we next examined the effect of cell therapy on myocyte cross-sectional area in both the remote and the peri-infarct myocardium. As expected, vehicle-receiving hearts were characterized by myocytes of greater dimensions and a reduction in the cardiomyocyte nuclear density as compared with sham-operated mice ($P<0.001$ for both comparisons; Figure 4D). These remodeling responses were attenuated in hearts that received CSC or SVP+CSC cell therapy.

Myocardial Repair

We next analyzed the effect of cell therapy on myocyte proliferation and apoptosis in the infarct border zone (Figure 5A and 5B). ANOVA detected an effect of cell therapy on both the histological outcomes ($P<0.01$). In multiple comparison analysis, CSCs surpassed SVPs with respect to cardiomyocyte proliferation, whereas combined treatment did not further improve the outcomes as compared with the best single therapy.

Importantly, cell therapy also exerted a supportive effect on the abundance of endogenous c-Kit$^+$ cells in the peri-infarct zone (ANOVA, $P<0.0001$; Figure 5C). About the classes of cells involved in the process, we observed an enhancement of the more primitive stem cells and progenitor cells (c-Kit$^+$ αSA$^-$), but not of myocyte precursors (c-Kit$^+$ αSA$^+$). In multiple comparison analyses, CSCs resulted to be more effective than SVPs in enhancing the number of primitive stem cells and progenitor cells. The combined cell transplantation did not surpass the effect of the best single treatment.

Vascular Repair

Immunohistochemistry analysis of peri-infarct microvasculature at 14 days post injection showed a higher density of capillaries and arterioles in cell-transplanted groups with respect to the vehicle group (ANOVA, $P<0.05$; Figure 5D and 5E). Multiple comparison analysis revealed that SVPs surpassed CSCs with regard to the microvascular density outcome. At 42 days, we observed that higher capillary density persisted in SVP- and SVP+CSC-treated hearts (Figure 5F). In addition, dual cell therapy promoted the growth of large arteriole density (Figure 5F). A superior proangiogenic capacity of SVPs versus CSCs was confirmed in an in vitro Matrigel assay (Online Figure IX).

Cumulative Cell Proliferation

To further investigate how the different cell therapies promote the processes of cardiomyogenesis and vasculogenesis, we administered a group of mice with the nucleoside analogue EdU.[19] EdU labeling in vivo provides an accumulative measure of new myocyte and vascular cell formation during the 2-week time post MI, whereas the Ki67$^+$ myocytes represent the ones that were still or had recently been in the cell cycle just before euthanization. Interestingly, results confirm that CSCs are better than SVPs in stimulating cardiomyocyte proliferation ($P<0.01$; Figure 6A and 6B). The combined transplantation of SVPs and CSCs did not show additive improvements over CSCs alone. These data, together with the finding of higher cardiomyocyte density and reduced cardiomyocyte cross-sectional area, suggest that CSC therapy stimulates myocyte proliferation in the infarcted heart.

About the process of vascularization, results confirmed that SVPs outperform CSCs in stimulating the proliferation of capillary endothelial cells ($P<0.05$ versus vehicle and CSCs; Figure 6C and 6D). In agreement with data showing an additive effect of dual therapy on arteriogenesis, we found that transplantation of SVPs and CSCs increases the density of EdU$^+$ vascular smooth muscle cells within arteriolar vessels ($P<0.05$; Figure 6C–6E).

Altogether, these data indicate that SVPs and CSCs exert prevalent actions on angiogenesis and myogenesis, respectively. Furthermore, dual cell therapy exerts additional benefit on the infarct size and arteriogenesis, but was similar to single cell therapy with regard to other outcomes. In the light of these differences, we performed additional studies in vitro to assess reciprocal, either positive or contrasting, interferences between the 2 cell populations.

Reciprocal Influence on Proliferation, Viability and Paracrine Activity

Although an interaction between transplanted and resident stem cells has been proposed,[15,30] little is known about the reciprocal influence of different donor cells. Therefore, we next performed in vitro coculture studies to determine whether SVPs and CSCs may affect each other with regard to several

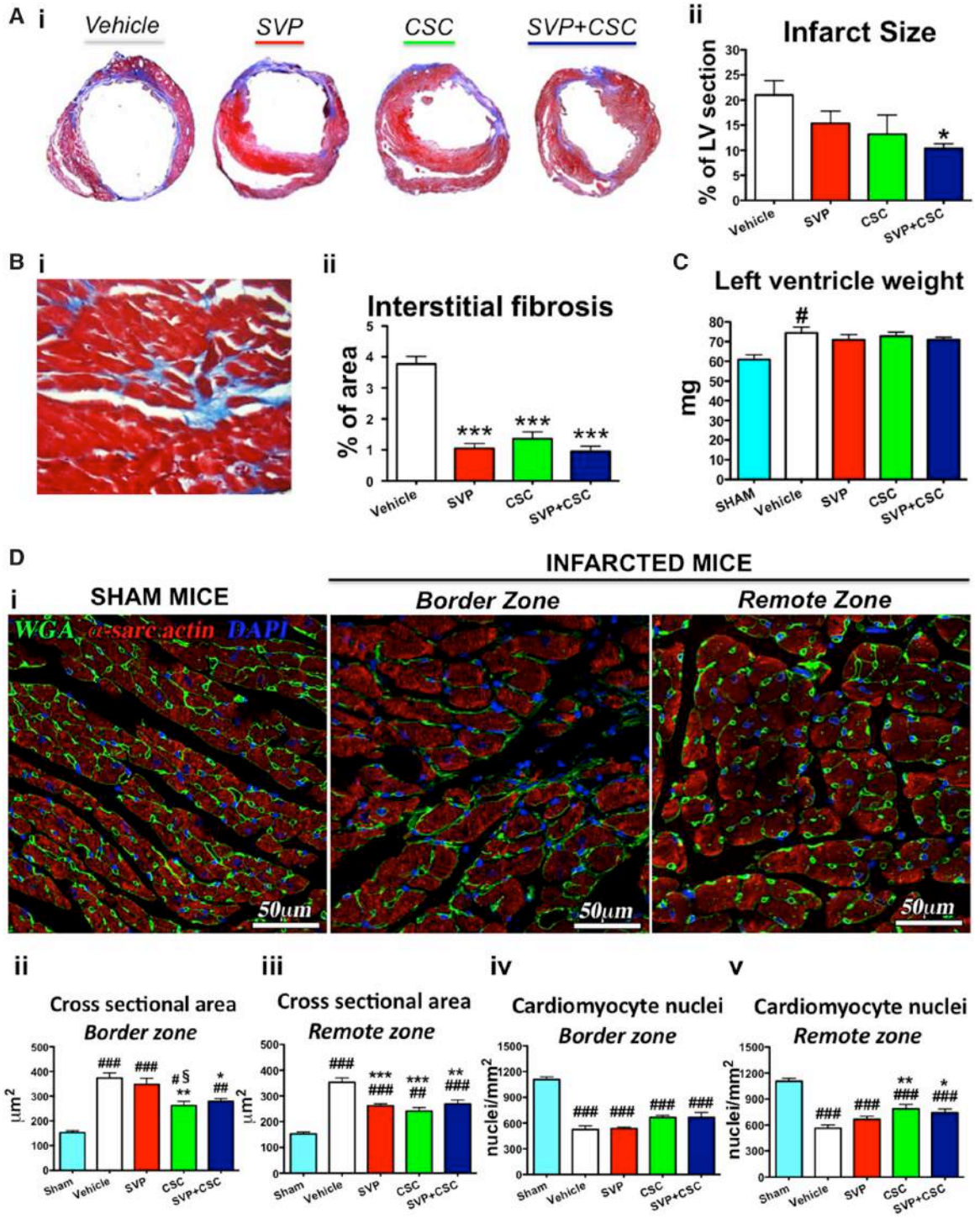

Figure 4. Morphometric evaluation of the left ventricle in mice 14 days post myocardial infarction (MI) and cell therapy.
A, Evaluation of infarct size. (i) Representative images of Azan Mallory staining in ventricular sections; collagen fibers are stained in blue (×12.5 magnification). (ii) Bar graphs summarize quantitative data of the percentage of the left ventricle occupied by the scar. **B**, Evaluation of interstitial fibrosis. (i) Representative images of Azan Mallory staining in ventricular sections (×200 magnification). (ii) Bar graphs summarize quantitative data of the percentage of the interstitial fibrotic area in the noninfarcted left ventricle. **C**, Left ventricular (LV) mass measurement after fixation of the whole heart with 4% paraformaldehyde and the following separation of the left ventricle from the atria and the right ventricle. **D**, Evaluation of cardiomyocyte hypertrophy. (i) Representative confocal images of wheat germ agglutinin (WGA; green), α-sarcomeric actin (red) and 4′,6-diamidino-2-phenylindole (DAPI; blue) in sham mice and in the peri-infarct (border zone) and remote myocardium (remote zone) of MI-mice. (ii–v) Histograms summarize quantitative data of cardiomyocyte cross-sectional area (ii and iii) and nuclear density (iv and v) in the border and remote myocardium. Data are presented as mean±SEM (n=3–4 sham, n=5–7 mice per each MI group). $^{\#}P<0.05$, $^{\#\#}P<0.01$, and $^{\#\#\#}P<0.001$ vs Sham; $^{*}P<0.05$, $^{**}P<0.01$, and $^{***}P<0.001$ vs vehicle; $^{\S}P<0.05$ vs saphenous vein–derived pericytes (SVP). CSC indicates cardiac stem cell.

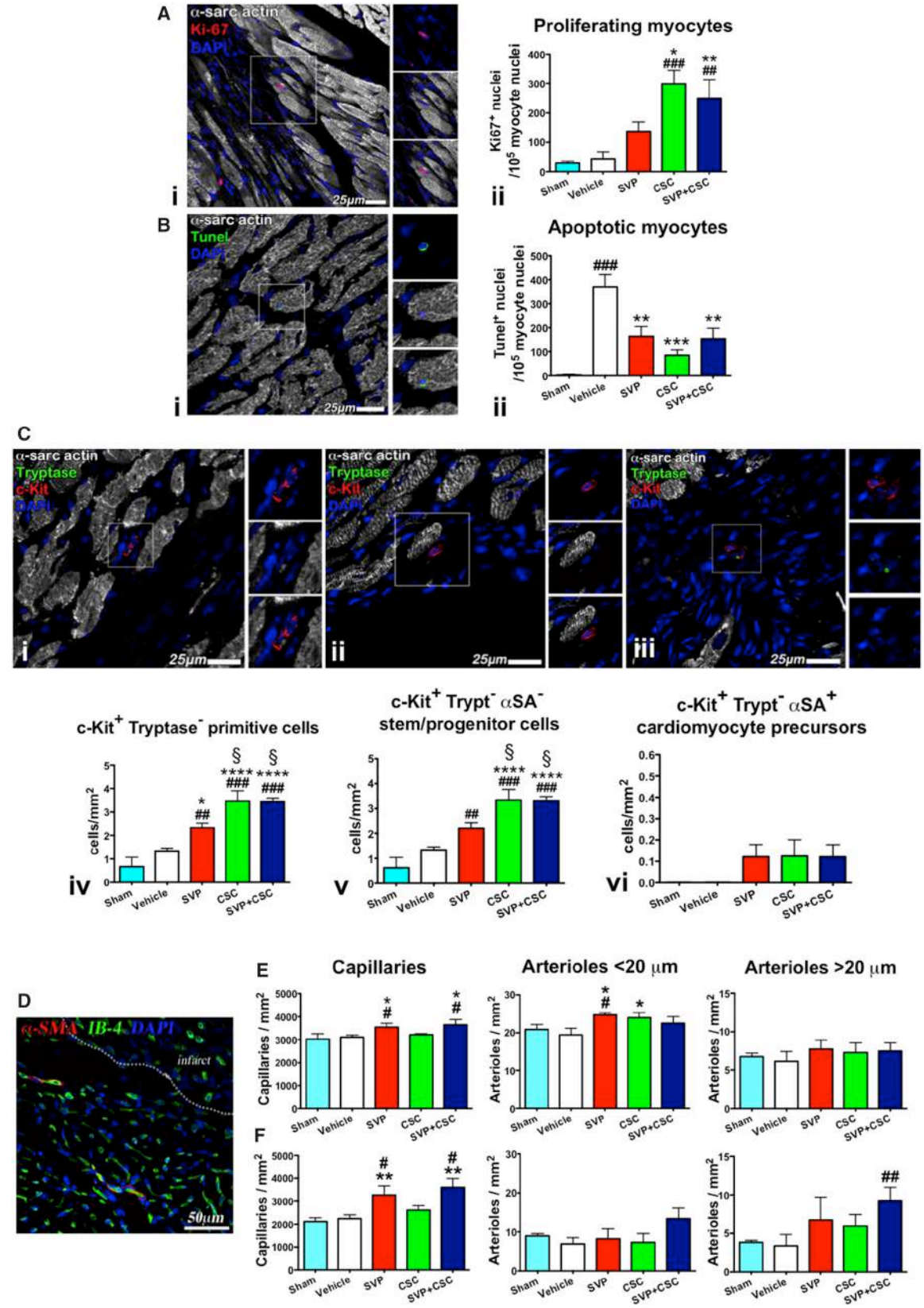

Figure 5. Effect of single or combined cell therapy on vascularization, cardiomyocyte proliferation/viability, and endogenous cardiac stem cell abundance. A and **B**, Cardiomyocytes in the peri-infarcted ventricles 14 days post myocardial infarction (MI). Confocal images of cardiomyocytes: **Ai**, the red fluorescence of Ki67 indicates proliferating cardiomyocytes; (**Bi**) the green fluorescence of terminal deoxynucleotidyl transferase dUTP nick end labeling (TUNEL) recognizes apoptotic cardiomyocytes. Cardiomyocyte cytoplasm is labeled by α-sarcomeric actin, represented in white. Nuclei are recognized by the blue fluorescence of 4′,6-diamidino-2-phenylindole (DAPI). Histograms summarize quantitative data of cardiomyocytes proliferation (**Aii**) and apoptosis (**Bii**) in the infarct border zone. **C**, (*Continued*)

Figure 5 Continued. Endogenous primitive cardiac stem cells in the peri-infarcted ventricle, 14 days post MI. **Upper**, Confocal images of (i) cardiac stem/progenitor cell (c-Kit$^+$ αSA$^-$ Tryptase$^-$) and cardiomyocyte precursor cell (c-Kit$^+$ αSA$^+$ Tryptase$^-$); (ii) cardiac stem/progenitor cell (c-Kit$^+$ αSA$^-$ Tryptase$^-$); (iii) cardiac mastocytes (c-Kit$^+$ Tryptase$^+$). c-Kit is stained in red, mast cell tryptase in green, α-sarcomeric actin in white, and nuclei in blue (DAPI). **Bottom**, Histograms summarize quantitative data of the density of (iv) total cKit-positive cardiac primitive cells, (v) stem and progenitor cells, and (vi) cardiomyocyte precursors in the infarct border zone of left ventricles. **D** to **F**, Angiogenesis in peri-infarcted ventricle. **D**, Representative epifluorescence image of isolectin B4 (IB4; green), α-smooth muscle actin (α-SMA; red) and DAPI (blue). Bar graphs show the density of capillaries and small (<20 μm in diameter) and large (>20 μm in diameter) arterioles, 14 days (**E**) and 42 days (**F**) post MI. Data are presented as mean±SEM (n=4 sham, n=5–7 mice per each MI group). $^{\#}P<0.05$, $^{\#\#}P<0.01$, and $^{\#\#\#}P<0.001$ vs Sham; $^{*}P<0.05$, $^{**}P<0.01$, $^{***}P<0.001$, and $^{****}P<0.0001$ vs vehicle; $^{\S}P<0.05$ vs saphenous vein–derived pericytes (SVP). CSC indicates cardiac stem cell.

functional properties. To distinguish 1 cell type from the other in a coculture system, SVPs were labeled with the cell tracker DiL. Uptake of DiL was confirmed in 95% of treated cells (Figure 7A).

We first compared the 2 cell populations with respect to proliferation rate and starvation-induced apoptosis, in single culture or coculture at a 1:1 ratio, which is the same proportion used for combined cell therapy in vivo. In both conditions, CSCs showed a higher incorporation rate of EdU ($P<0.01$ versus SVPs; Figure 7B) and a higher propensity to undergo starvation-induced apoptosis ($P<0.05$ versus SVPs; Figure 7C). Moreover, we verified the reciprocal effect on viability in a coculture chamber system where the 2 cell populations were exposed to the same starvation medium (serum-free EGM-2 [endothelial cell

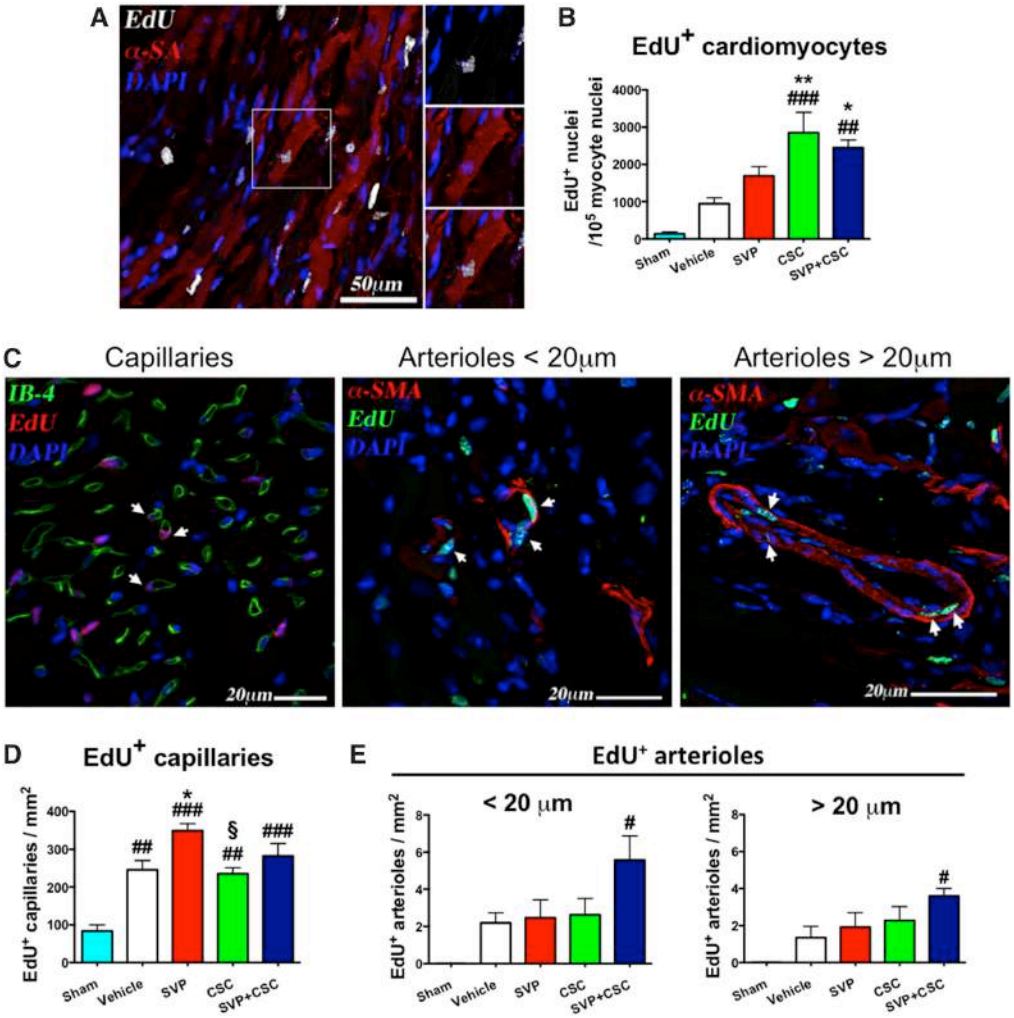

Figure 6. Cardiomyogenesis and vasculogenesis in the left ventricle 14 days post myocardial infarction (MI). and cell therapy. **A**, Representative confocal image of an 5-ethynyl-2′-deoxyuridine (EdU)$^+$ cardiomyocyte in the peri-infarct region. Nuclear EdU is depicted in white, whereas cardiomyocyte cytoplasm is labeled by α-sarcomeric actin (α-SA), in red fluorescence. **B**, Bar graphs show quantitative data of EdU$^+$ cardiomyocyte nuclei in the peri-infarct myocardium. **C**, Representative confocal images of capillaries and small and large arterioles in the peri-infarct myocardium. Isolectin-B4 (IB4) is shown in green, α-smooth muscle actin (α-SMA) in red, whereas nuclear EdU is shown in red or in green. 4′,6-Diamidino-2-phenylindole (DAPI) is represented in blue. Cells positive for EdU are identified by white arrows. **D** to **E**, Bar graphs show the density of EdU$^+$ capillaries (**D**) and small (<20 μm in diameter) and large (>20 μm in diameter) arterioles (**E**) in the peri-infarct myocardium. Data are presented as mean±SEM (n=3 sham, n=6 mice per each MI group). $^{\#}P<0.05$, $^{\#\#}P<0.01$, and $^{\#\#\#}P<0.001$ vs. Sham; $^{*}P<0.05$ and $^{**}P<0.01$ vs vehicle; $^{\S}P<0.05$ vs saphenous vein–derived pericytes (SVP). CSC indicates cardiac stem cell.

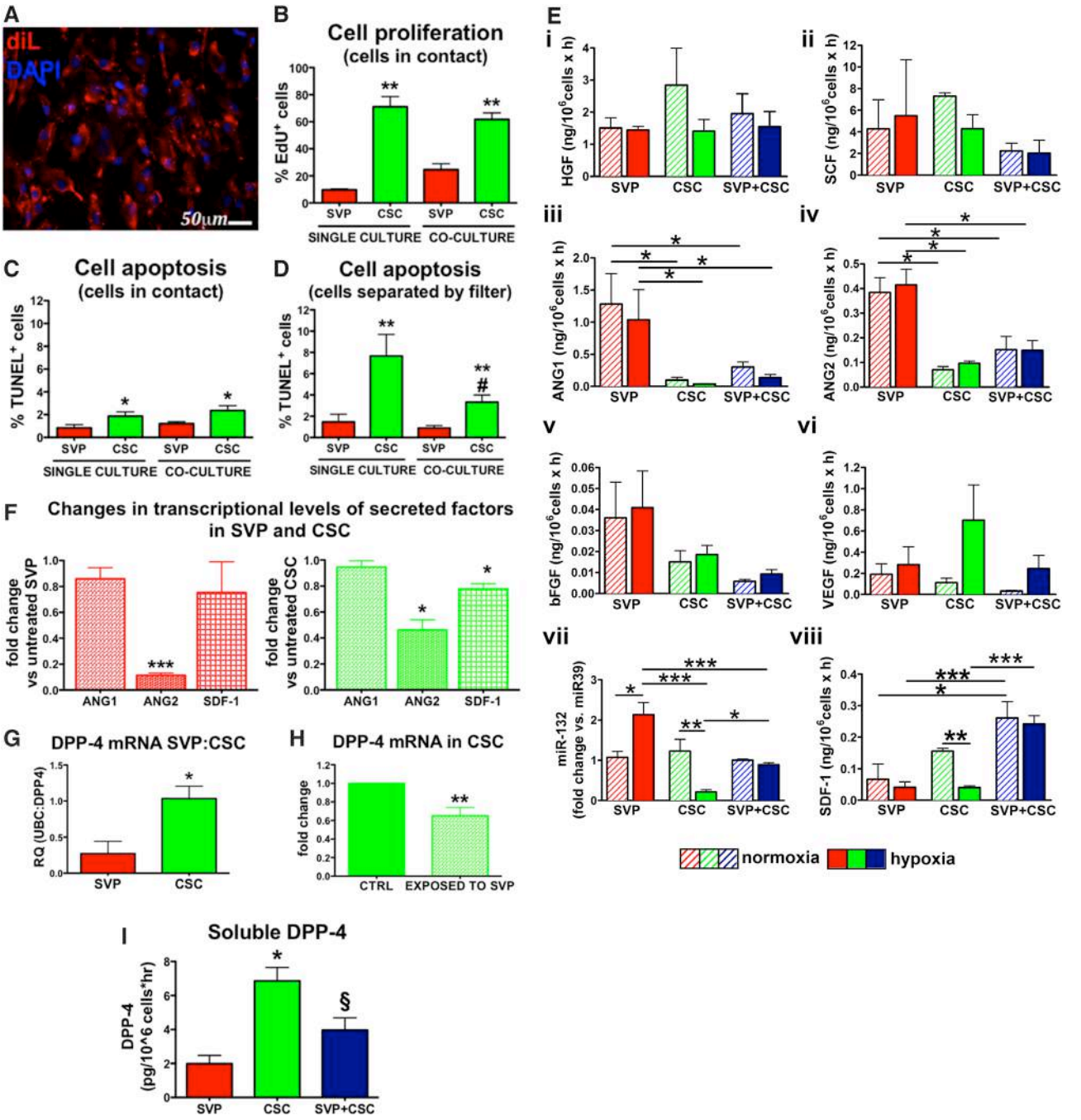

Figure 7. In vitro interaction between cardiac stem cells (CSCs) and saphenous vein–derived pericytes (SVPs) and cell secretome. For coculture experiments, SVPs have been labeled with the cell tracker VyBrant DiL (from Life Technologies). **A**, A representative image of labeled SVPs. The efficiency of labeling is 95%. **B**, Cell proliferation. Histograms show the percentage of 5-ethynyl-2′-deoxyuridine (EdU)+ CSCs and SVPs in single or combined-culture (seeding cells following a 1:1 ratio), after a 20-hour long incubation in medium supplemented with EdU. **C** and **D**, Cell apoptosis. Histograms show the percentage of apoptotic cells, in single or combined culture, after a starvation of 48 hours in EGM-2 (endothelial cell growth medium-2) serum-free medium. Cells in coculture were in contact (C) or separated by a semipermeable membrane (**D**). Data are presented as mean±SEM (n=3 per group). **P*<0.05, ***P*<0.01 vs saphenous vein–derived pericytes (SVPs); #*P*<0.05 vs CSCs in single culture. **E**, Secretome of SVPs, CSCs, and cocultures of SVPs+CSCs, in normoxia (20% oxygen) and hypoxia (2%). (i–viii) Histograms show the amount of secreted factors normalized for the volume of the collected supernatant, cell number, and time of incubation. (vii) miR-132 released in cell supernatant. For each group of cells, fold change of the normoxic culture is reported. Data are presented as mean±SEM (n=3 per group). **P*<0.05, ***P*<0.01, and ****P*<0.001. **F**, Transcriptional changes of angiopoietins (ANGs) and stromal cell–derived factor-1α (SDF-1α) in CSCs and SVPs (both n=3) exposed for 6 hours to each other conditioned medium. Histograms show the n-fold change with respect to untreated cells. Data are presented as mean±SEM. **P*<0.05 and ****P*<0.001 vs untreated cells. **G**, Dipeptidyl peptidase 4 (DPP-4) mRNA expressional levels in SVPs and CSCs assessed by quantitative polymerase chain reaction analysis. Histograms show the n-fold change with respect to CSCs. Data are presented as mean±SEM (n=4 CSCs, 5 SVPs). **P*<0.05 vs CSCs. **H**, Transcriptional changes of DPP-4 in CSCs (n=4) exposed for 6 hours to SVP conditioned medium. Histograms show the n-fold change with respect to untreated cells. Data are presented as mean±SEM. ***P*<0.01 vs untreated cells. **I**, Histograms show the amount of secreted DPP-4 in supernatants of SVPs, CSCs, and cocultures of SVPs+CSCs, in hypoxia. Data are normalized for the volume of the collected supernatant, cell number, and time of incubation. Data are presented as mean±SEM (n=4 per group). **P*<0.05 vs SVPs, §*P*<0.05 vs CSCs. bFGF indicates basic fibroblast growth factor; HGF, hepatocyte growth factor; SCF, stem cell factor; and VEGF, vascular endothelial growth factor.

growth medium-2 from Lonza]), but kept separated by a semipermeable membrane to avoid mutual contacts. As shown in Figure 7D, the abundance of terminal deoxynucleotidyl transferase dUTP nick end labeling–positive CSCs was higher than that of SVPs, either when cells were kept alone or together ($P<0.01$ for both comparisons), thus confirming the results of the mixed coculture experiment described above. Noteworthy, cell coincubation halved the fraction of terminal deoxynucleotidyl transferase dUTP nick end labeling+ CSCs ($P<0.05$ versus single culture), thus suggesting that SVPs secrete factors that increase CSC viability. Altogether these in vitro data indicate that the mixture of different stem cells does not alter their proliferation rate and resistance to starvation, with the latter property being eventually improved if cells are not in contact.

Transplanted cells secrete combinations of trophic factors that modulate the molecular composition of the ischemic environment to evoke healing responses.[31,32] However, to the best of our knowledge, it remains unknown whether different stem cell types in combination may influence each other's secretome. To investigate these paracrine interactions, we measured growth factors and cytokines secreted by SVPs and CSCs in single culture or coculture under normoxic or hypoxic conditions. The secretory capacity was calculated by normalizing the amount of a given secreted factor by the cell number, which was assessed at the end of the collection period.

We found that SVPs and CSCs release similar levels of hepatocyte growth factor and stem cell factor, with no substantial changes in normoxia versus hypoxia or monoculture versus coculture (Figure 7Ei and 7Eii). Noteworthy, SVPs secrete the proangiogenic factors angiopoietin 1 (ANG1) and 2 (ANG2) at higher concentrations than CSCs ($P<0.05$ and 0.01, respectively; Figure 7Eiii and 7Eiv). A similar trend was observed with basic fibroblast growth factor although the difference did not reach statistical significance (Figure 7Ev). Interestingly, the secretion of angiopoietins and basic fibroblast growth factor by cells in coculture was lower than the average of the 2 cell preparations, thus suggesting a negative reciprocal interference. Moreover, hypoxia induced an increase in the secretion of vascular endothelial growth factor by CSCs, but this effect was not observed in the SVP-CSC coculture (Figure 7Evi). Proangiogenic growth factors induce miR-132 expression in vascular cells via activation of the transcription factor cAMP response element-binding protein.[33] Furthermore, we have previously demonstrated that SVPs abundantly express and release miR-132 and that secreted miR-132 is in part responsible for the SVP ability to induce reparative angiogenesis and reduce infarct size after transplantation in the mouse heart.[12] Therefore, we next investigated the reciprocal interference of SVPs and CSCs on miR-132 secretion under normoxia or hypoxia. Interestingly, we found an opposite behavior of the 2 cell types: in fact, hypoxia increases the miR-132 levels in SVP conditioned medium ($P<0.05$ versus normoxia) as reported by us previously,[12] but reduces miR-132 in CSC conditioned medium ($P<0.01$ versus normoxia; Figure 7Evii). However, we observed an additive effect of the cell coculture on the secretion of stromal cell–derived factor 1α (SDF-1α) under normoxia (ANOVA, $P<0.05$; Figure 7Eviii). This phenomenon was more evident under hypoxia (ANOVA, $P<0.01$), being the SDF-1α secretion by cocultured cells greater than the sum of individual cell culture systems (Figure 7Eviii). Altogether, these data newly indicate a complex interactive behavior at the level of secretome, which may result in attenuated secretion of vascular endothelial growth factor, ANG1, ANG2, basic fibroblast growth factor, and miR-132 in comparison with the prominent cell producer, but synergic release of SDF-1α.

To determine whether these phenomena are transcriptionally modulated, we performed quantitative polymerase chain reaction analyses of angiopoietins and SDF-1 mRNA levels in SVPs and CSCs before and after 6-hour exposure to each other's conditioned medium. As shown in Figure 7F, conditioned media reduced the expression of ANG2 in both the cell types ($P<0.001$ for SVPs, $P<0.05$ for CSCs versus the respective cell control exposed to unconditioned medium), whereas ANG1 remained unaltered. In addition, CSCs exposed to SVP conditioned medium showed reduced SDF-1α mRNA levels ($P<0.05$ versus CSCs exposed to unconditioned medium). These data newly show a transcriptional interference with respect to ANG2 and SDF-1. However, while ANG2 expression was consistently reduced at mRNA and protein level, the increase in SDF-1α content in coculture media cannot be attributed to the induction of gene transcription, but rather to an increase in secretion rate.

Chemokine availability in the extracellular compartment is also dictated by the activity of degrading enzymes. Dipeptidyl peptidase-4 (DPP-4), also known as adenosine deaminase complexing protein 2 or CD26 (EC 3.4.14.5), cleaves a spectrum of proline- or alanine-containing chemokines, including SDF-1α. Importantly, increased SDF-1α availability has been proposed to mediate the cardioprotective and proangiogenic activity of DPP-4 inhibitors in MI models.[34] As shown in Figure 7G, quantitative polymerase chain reaction analysis shows that DPP-4 is more expressed by CSCs than SVPs ($P<0.05$). Furthermore, DPP-4 is downregulated in CSCs exposed to SVP conditioned medium ($P<0.01$; Figure 7H). In keeping with transcriptional results, ELISA of conditioned media confirmed higher DPP-4 secretion by CSCs ($P<0.05$ versus SVPs), which is attenuated when CSCs are cocultured with SVPs ($P<0.05$ versus CSCs alone; Figure 7I).

Functional Impact of SVP and CPC Secretomes on Endothelial Cells, Cardiomyocytes, and CSCs

To investigate the effect of secretome on specific target cells, we first tested the proangiogenic capacity of SVPs, CSCs, and their coculture in a Matrigel endothelial network assay. As shown in Figure 8A, ANOVA detected a positive effect of conditioned media on network formation by human umbilical vein endothelial cells ($P<0.05$ versus unconditioned medium), but no additive effect was observed with SVP-CSC combination as compared with single conditioned media. Instead, only SVP and SVP+CSC conditioned media are able to stimulate the proliferation of human umbilical vein endothelial cells ($P<0.05$ versus EGM-2), with this effect being refused to CSCs (Figure 8B).

We next investigated the protective effect of SVP and CSC secreted factors against apoptosis after simulated ischemia/reoxygenation in isolated adult rat cardiomyocytes. The purity of the cell preparation was assessed by staining with α-sarcomeric actinin antibody (Figure 8C). As shown in Figure 8D, the simulated ischemia/reoxygenation protocol effectively induces cardiomyocyte apoptosis compared with normoxia. We found that the secretome of each cell population is able to protect

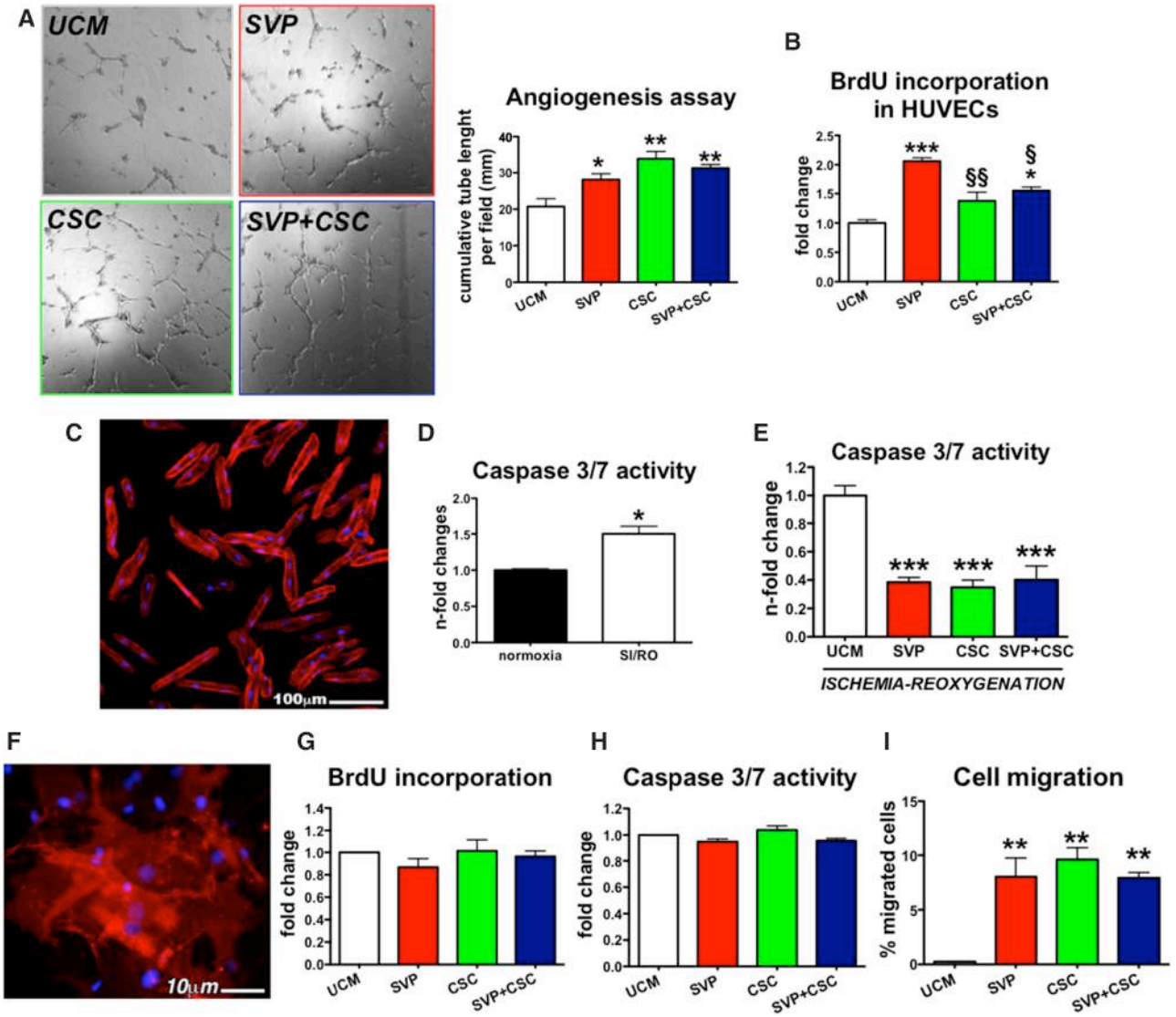

Figure 8. Functional impact of the secretome(s) on endothelial cells, cardiomyocytes, and cardiac stem cells. A, Angiogenesis assay. Matrigel assay: Representative phase-contrast optical images of human umbilical vein endothelial cells (HUVECs) forming tubular networks when cultured for 6 hours on Matrigel substrate, with EGM-2 (endothelial cell growth medium-2) media conditioned by saphenous vein–derived pericytes (SVPs), cardiac stem cells (CSCs), or SVPs+CSCs or unconditioned medium (UCM; magnification ×50). Histograms summarize quantitative data of the tubes length per field. n=5 per each group. **B**, Effect of cell secretome on HUVECs proliferation. Histograms summarize quantitative data of cell proliferation (measured as incorporation of BrdU [5-bromo-2'-deoxyuridine]) in HUVECs cultured in medium conditioned by SVPs, CSCs, or SVPs+CSCs or UCM for 40 hours, in the presence of BrdU. Data are fold changes of UCM. n=3 per group. **C** to **E**, Simulated ischemia reoxygenation (SI/RO) injury on isolated adult rat cardiomyocytes. **C**, Confocal image of cardiomyocytes in culture. Cardiomyocytes cytoplasm is labeled by α-sarcomeric actinin stained in red, whereas nuclei are shown in blue (4′,6-diamidino-2-phenylindole [DAPI]). **D**, Histograms summarize quantitative data of apoptosis (measured as caspase 3/7 activity) in cardiomyocytes after the SI/RO compared with control cells cultured in basal conditions. **E**, Histograms summarize quantitative data of apoptosis (measured as caspase 3/7 activity) in cardiomyocytes subjected to SI/RO and cultured in medium conditioned by SVPs, CSCs, or SVPs+CSCs or UCM. n=3 for each group. **F** to **I**, Effects of cell secretome on mouse Sca-1$^+$ cardiac stem cells. **F**, Epifluorescence image of Sca-1$^+$ cardiac stem cells in culture. Sca-1 on cell surface is stained in red, whereas nuclei (DAPI) are shown in blue. **G**, Proliferation. Histograms summarize quantitative data of cell proliferation (measured as incorporation of BrdU) in Sca-1$^+$ cells cultured in medium conditioned by SVPs, CSCs, or SVPs+CSCs or UCM for 16 hours, in the presence of BrdU. Data are fold change of UCM. **H**, Apoptosis. Histograms summarize quantitative data of cell apoptosis (measured as caspase 3/7 activity) in Sca-1$^+$ cells cultured in medium conditioned by SVPs, CSCs, or SVPs+CSCs or UCM for 48 hours, in serum-free medium; data are fold change of UCM. n=3 for each group. **I**, Cell migration. Histograms show the percentage of Sca-1$^+$ cells migrated toward SVPs, CSCs, or SVPs+CSCs conditioned medium or UCM, during a period of 8 hours. n=3 per group. Data are presented as mean±SEM. *P<0.05, **P<0.01, and ***P<0.001 vs UCM; §P<0.05 and §§P<0.01 vs SVPs.

rat cardiomyocytes from apoptosis (P<0.001 versus unconditioned medium for both comparisons), with no additive effect when using the coculture conditioned media (Figure 8E).

Finally, we verified the effects of conditioned media on murine CSCs. Figure 8F shows a typical immunofluorescence microscopy image of Sca-1$^+$ cells isolated from the mouse heart.[35] As illustrated in Figure 8G and 8H, conditioned media did not affect Sca-1$^+$ cell proliferation or apoptosis. However, they markedly stimulated the migration of murine Sca-1$^+$ cells in a Boyden chamber assay (P<0.01 for both comparisons),

with no additive effect being observed after stimulation with the coculture conditioned media (Figure 8I).

Discussion

This study provides new important insights into the optimization of cell therapy for cardiac repair using populations with complementary healing properties. We show that, by combining the capacities of human CSCs to promote cardiomyogenesis, via recruitment of endogenous stem cells and induction of cardiomyocyte reentry into the cell cycle, and of human SVPs to boost vascularization, it becomes possible to obtain additive reduction of the scar size in a murine model of MI. However, dual cell therapy did not surpass the best-performing cell population with regard to other outcome measures, including contractility and pressure indexes, myocyte remodeling, and interstitial fibrosis. In addition, results newly show a previously unforeseen paracrine interaction between the 2 cell populations.

Feasibility and efficacy of CSCs have been already tested in clinical trials.[2–5] Nevertheless, there are multiple challenges to the use of autologous CSCs, including among the others the need of a cardiac biopsy. We have now developed a clinical-grade version of the SVP expansion protocol from discarded human veins for use at the GMP facilities of NHS Blood and Transplant, which is a Special Health Authority with responsibility for managing the supply of blood, organs, and tissues in the UK. Therefore, SVPs represent a practical alternative as well as a convenient complement to CSCs for cardiac cell therapy.

There are few antecedent studies investigating combinatory cell therapy approaches. A recent report by Williams et al[1] combining human CSCs and bone marrow MSCs in a swine model of MI showed that each cell therapy reduces MI size relative to placebo, with the MI size reduction being 2-fold greater in combination versus either cell therapy alone. These results are similar to ours; however, in Williams' report there was a substantial improvement in LV chamber compliance and contractility by dual cell therapy, whereas we could not observe additional benefit over single therapy. It should be noted that in Williams's study the engraftment of CSCs and MSCs in the combination group was 7-fold greater than in either cell group administered alone,[1] whereas we did not observe such a remarkable effect. Besides the different animal models used (pharmacologically immunosuppressed pigs undergoing ischemia/reperfusion versus immunodeficient mice undergoing permanent coronary artery occlusion), the 2 studies also differ in terms of time points for cell therapy injection after MI induction: whereas in Williams' study cells were intramyocardially injected at 14 days post MI, we performed cell therapy at the occasion of coronary artery occlusion. The late application might account for a better cell engraftment and contractility improvement. Additional reasons for the discrepancy in functional outcomes remain to be elucidated.

Direct contact and paracrine signaling between cells induce functional changes and may also influence the susceptibility to a variety of stressors. In addition, competitive interaction between stem cells within their native niches reportedly results in survival of the fittest stem cells and death of the more susceptible cells.[36] Expanding these concepts to cell therapy, the outcome of dual cell delivery may depend on the balance between cooperative and competitive interactions. We ruled out any negative effect of pooling SVPs and CSCs before intramyocardial delivery. In addition, we observed improved cell viability when SVPs and CSCs were cultured in the same in vitro system, but kept separated by a filter. Noteworthy, when comparing the secretome of single and dual cell products, we observed important changes at transcriptional and post-transcriptional level. In particular, SVPs secrete larger amounts of angiogenic factors, such as angiopoietins, basic fibroblast growth factor, and miR-132, as compared with CSCs. However, angiocrine secretion per cell unit was reduced below the average of each cell population when SVPs and CSCs were cultured together, thus suggesting an inhibitory effect. In both cell populations, this inhibition is likely to occur at transcriptional level for ANG2 but not for ANG1, as indicated by the reduction of ANG2 mRNA levels when cells are exposed to media conditioned by the other cell type. However, analysis of the secretome indicates that SDF-1α release is remarkably increased in the coculture system. We verified that in both cell populations this modulation occurs at post-transcriptional level and may involve a reduction in SDF-1αdegradation by DDP4. Previous studies have shown that SDF-1α plays a key role in recruiting bone marrow–derived stem cells to the sites of vascular and myocardial injury.[37,38] Furthermore, transplantation of cardiac fibroblasts, MSCs, or skeletal myoblasts genetically engineered to express high constitutive levels of SDF-1αreportedly reduces cardiomyocyte death, increases vascular density, and improves cardiac function in preclinical models of myocardial ischemia.[37,39,40] Likewise, early intravenous infusion of hypoxia-preconditioned, cardiosphere-derived c-Kit$^+$ Lin$^-$ cells induces general cardiac benefit in a murine model of MI.[41] This effect was attributed to an activation of the SDF-1α/CXCR4 axis, as both cell engraftment and functional improvements from cell therapy were inhibited by preincubation of c-Kit$^+$ Lin$^-$ cells with MD-3100, a CXCR4 antagonist.[41] There is also initial evidence that prolongation of SDF-1α expression at the time of acute MI by infusion of SDF-1α–engineered MSCs leads to the recruitment of small-size, myosin, and connexin-45–positive cardiac cells that are capable of depolarizing and may represent a population of resident stem cells.[42]

Although direct injection into the myocardium represents the preferred delivery route to maximize stem cell retention in the infarcted heart, survival and long-term engraftment remain rather modest.[43] Furthermore, different cell types might have dissimilar engraftment kinetics, depending on their ability to resist to the harsh environment of an ischemic heart and to establish retaining contacts with recipient's cells. Here, we newly show that transplanted SVPs are endowed with higher incorporation rate compared with CSCs. Furthermore, after combined injection, the 2 cell types were localized distant from each other in the recipient's heart. As a consequence, local promotion of cardiomyocyte repair by CSCs may remain temporally and spatially disconnected from the SVP-induced neovascularization. Implemented delivery systems and tissue engineering approaches, allowing a stronger interaction in vivo, might be necessary to integrate those distinct reparative mechanisms into a synergic action.

Dual cell therapy delivered significant benefits in term of reduction of infarct size and arteriogenesis. The molecular and cellular mechanisms for scar size reduction with cell therapy remain controversial. It is likely that each cell population used in the present study has contributed in a distinct and complementary manner, rather than through cooperation within a specific mechanism. Differentiation of CSCs into cardiomyocytes was a rare event,

whereas SVPs did not show any cardiomyogenic activity either in vitro or in vivo. Both SVPs and CSCs inhibit cardiomyocyte apoptosis and CSCs uniquely stimulate adult cardiomyocytes to re-enter the cell cycle. Prevention of cardiomyocyte loss in the area at risk and production of new cardiomyocytes may have therefore concurred in reducing the scar dimensions. The ability of cell therapy to stimulate endogenous CSCs to proliferate and differentiate is emerging as an exciting new mechanism of action.[30] We newly report that intramyocardial injection of SVPs or CSCs, as a single or combined therapy, increases the abundance of primitive c-Kit$^+$ cells in the peri-infarct zone and that the conditioned medium of the 2 populations exerts a potent chemoattractant activity on murine CSCs, without influencing their proliferation or viability. Vasculogenesis and enhanced blood supply to areas of hibernating myocardium are relevant in limiting infarct extension. Our study indicates that SVP transplantation helps the development of capillary and arteriolar coronary vessels in the infarct border zone, with dual cell therapy enhancing the arteriogenic effect. SVPs express recognition binding sites that facilitate perivascular engraftment in vivo, through the establishment of robust interactions with cadherin-based adherens junctions on the coronary endothelium.[15] Here, we report the indirect support of transplanted SVPs on vascularization. In fact, we could not find evidence of SVP or CSC differentiation into endothelial cells. Nonetheless, single cell therapy with SVPs and dual cell therapy with SVPs and CSCs increased the proliferation of capillary endothelial cells and vascular smooth muscle cells, thus resulting in an expansion of large arterioles.

In conclusion, this study is the first to document the functional, histological, and molecular interaction of combined cell therapy with human CSCs and SVPs. The 2 cell populations are therapeutically effective in a mouse model of MI and in combination they work better to reduce infarct size and collateralization. Combinatory approaches using stem cells from discarded surgical tissue may open unprecedented opportunities for cardiac repair.

Sources of Funding

This study was supported by (1) human pericyte progenitor cells and cardiac progenitor cells for specialized stimulation of neovascularization and cardiomyogenesis of the infarcted heart, British Heart Foundation (BHF) Project Grant; (2) manufacture scale up of human pericyte progenitor cells for regenerative medicine, MRC Translational Stem Cell Research Grant; (3) Biomedical Research Unit in Cardiovascular Disease (lead for Regenerative Medicine workpackage); National Institute Health Research Biomedical Research Unit; (4) preclinical trial with human pericyte progenitors in a large animal model of myocardial infarction, BHF special project grant; and (5) BHF Centre of Regenerative Medicine.

Disclosures

None.

References

1. Williams AR, Hatzistergos KE, Addicott B, McCall F, Carvalho D, Suncion V, Morales AR, Da Silva J, Sussman MA, Heldman AW, Hare JM. Enhanced effect of combining human cardiac stem cells and bone marrow mesenchymal stem cells to reduce infarct size and to restore cardiac function after myocardial infarction. *Circulation*. 2013;127:213–223. doi: 10.1161/CIRCULATIONAHA.112.131110.
2. Chugh AR, Beache GM, Loughran JH, Mewton N, Elmore JB, Kajstura J, Pappas P, Tatooles A, Stoddard MF, Lima JA, Slaughter MS, Anversa P, Bolli R. Administration of cardiac stem cells in patients with ischemic cardiomyopathy: the SCIPIO trial: surgical aspects and interim analysis of myocardial function and viability by magnetic resonance. *Circulation*. 2012;126:S54–S64. doi: 10.1161/CIRCULATIONAHA.112.092627.
3. Bolli R, Chugh AR, D'Amario D, et al. Cardiac stem cells in patients with ischaemic cardiomyopathy (SCIPIO): initial results of a randomised phase 1 trial. *Lancet*. 2011;378:1847–1857. doi: 10.1016/S0140-6736(11)61590-0.
4. Makkar RR, Smith RR, Cheng K, Malliaras K, Thomson LE, Berman D, Czer LS, Marbán L, Mendizabal A, Johnston PV, Russell SD, Schuleri KH, Lardo AC, Gerstenblith G, Marbán E. Intracoronary cardiosphere-derived cells for heart regeneration after myocardial infarction (CADUCEUS): a prospective, randomised phase 1 trial. *Lancet*. 2012;379:895–904. doi: 10.1016/S0140-6736(12)60195-0.
5. Malliaras K, Makkar RR, Smith RR, Cheng K, Wu E, Bonow RO, Marbán L, Mendizabal A, Cingolani E, Johnston PV, Gerstenblith G, Schuleri KH, Lardo AC, Marbán E. Intracoronary cardiosphere-derived cells after myocardial infarction: evidence of therapeutic regeneration in the final 1-year results of the CADUCEUS trial (CArdiosphere-Derived aUtologous stem CElls to reverse ventricULar dySfunction). *J Am Coll Cardiol*. 2014;63:110–122. doi: 10.1016/j.jacc.2013.08.724.
6. Ellison GM, Vicinanza C, Smith AJ, et al. Adult c-kit(pos) cardiac stem cells are necessary and sufficient for functional cardiac regeneration and repair. *Cell*. 2013;154:827–842. doi: 10.1016/j.cell.2013.07.039.
7. Torella D, Ellison GM, Nadal-Ginard B. Adult c-kit(pos) cardiac stem cells fulfill Koch's postulates as causal agents for cardiac regeneration. *Circ Res*. 2014;114:e24–e26. doi: 10.1161/CIRCRESAHA.113.303313.
8. van Berlo JH, Kanisicak O, Maillet M, Vagnozzi RJ, Karch J, Lin SC, Middleton RC, Marbán E, Molkentin JD. c-kit+ cells minimally contribute cardiomyocytes to the heart. *Nature*. 2014;509:337–341. doi: 10.1038/nature13309.
9. The Lancet E. Expression of concern: the SCIPIO trial. *Lancet*. 2014;383:1279.
10. Magenta A, Avitabile D, Pompilio G, Capogrossi MC. c-kit-Positive cardiac progenitor cells: the heart of stemness. *Circ Res*. 2013;112:1202–1204. doi: 10.1161/CIRCRESAHA.113.301317.
11. Vono R, Spinetti G, Gubernator M, Madeddu P. What's new in regenerative medicine: split up of the mesenchymal stem cell family promises new hope for cardiovascular repair. *J Cardiovasc Transl Res*. 2012;5:689–699. doi: 10.1007/s12265-012-9395-2.
12. Katare R, Riu F, Mitchell K, Gubernator M, Campagnolo P, Cui Y, Fortunato O, Avolio E, Cesselli D, Beltrami AP, Angelini G, Emanueli C, Madeddu P. Transplantation of human pericyte progenitor cells improves the repair of infarcted heart through activation of an angiogenic program involving micro-RNA-132. *Circ Res*. 2011;109:894–906. doi: 10.1161/CIRCRESAHA.111.251546.
13. Chen CW, Okada M, Proto JD, Gao X, Sekiya N, Beckman SA, Corselli M, Crisan M, Saparov A, Tobita K, Péault B, Huard J. Human pericytes for ischemic heart repair. *Stem Cells*. 2013;31:305–316. doi: 10.1002/stem.1285.
14. Nees S, Weiss DR, Juchem G. Focus on cardiac pericytes. *Pflugers Arch*. 2013;465:779–787. doi: 10.1007/s00424-013-1240-1.
15. Campagnolo P, Cesselli D, Al Haj Zen A, Beltrami AP, Kränkel N, Katare R, Angelini G, Emanueli C, Madeddu P. Human adult vena saphena contains perivascular progenitor cells endowed with clonogenic and proangiogenic potential. *Circulation*. 2010;121:1735–1745. doi: 10.1161/CIRCULATIONAHA.109.899252.
16. Beltrami AP, Cesselli D, Bergamin N, et al. Multipotent cells can be generated in vitro from several adult human organs (heart, liver, and bone marrow). *Blood*. 2007;110:3438–3446. doi: 10.1182/blood-2006-11-055566.
17. Avolio E, Gianfranceschi G, Cesselli D, et al. Ex vivo molecular rejuvenation improves the therapeutic activity of senescent human cardiac stem cells in a mouse model of myocardial infarction. *Stem Cells*. 2014;32:2373–2385. doi: 10.1002/stem.1728.
18. Bearzi C, Rota M, Hosoda T, et al. Human cardiac stem cells. *Proc Natl Acad Sci U S A*. 2007;104:14068–14073. doi: 10.1073/pnas.0706760104.
19. Eulalio A, Mano M, Dal Ferro M, Zentilin L, Sinagra G, Zacchigna S, Giacca M. Functional screening identifies miRNAs inducing cardiac regeneration. *Nature*. 2012;492:376–381. doi: 10.1038/nature11739.
20. Asahara T, Murohara T, Sullivan A, Silver M, van der Zee R, Li T, Witzenbichler B, Schatteman G, Isner JM. Isolation of putative progenitor endothelial cells for angiogenesis. *Science*. 1997;275:964–967.
21. Lin CS, Lue TF. Defining vascular stem cells. *Stem Cells Dev*. 2013;22:1018–1026. doi: 10.1089/scd.2012.0504.
22. Torsney E, Xu Q. Resident vascular progenitor cells. *J Mol Cell Cardiol*. 2011;50:304–311. doi: 10.1016/j.yjmcc.2010.09.006.
23. Corselli M, Chen CW, Sun B, Yap S, Rubin JP, Péault B. The tunica adventitia of human arteries and veins as a source of mesenchymal stem cells. *Stem Cells Dev*. 2012;21:1299–1308. doi: 10.1089/scd.2011.0200.

24. Diaz-Flores L, Gutierrez R, Garcia MP, Saez FJ, Diaz-Flores L Jr, Valladares F, Madrid JF. CD34+ stromal cells/fibroblasts/fibrocytes/telocytes as a tissue reserve and a principal source of mesenchymal cells. Location, morphology, function and role in pathology. *Histol Histopathol*. 2014;29:831–870.
25. Smits AM, van Vliet P, Metz CH, Korfage T, Sluijter JP, Doevendans PA, Goumans MJ. Human cardiomyocyte progenitor cells differentiate into functional mature cardiomyocytes: an in vitro model for studying human cardiac physiology and pathophysiology. *Nat Protoc*. 2009;4:232–243. doi: 10.1038/nprot.2008.229.
26. Penicka M, Widimsky P, Kobylka P, Kozak T, Lang O. Images in cardiovascular medicine. Early tissue distribution of bone marrow mononuclear cells after transcoronary transplantation in a patient with acute myocardial infarction. *Circulation*. 2005;112:e63–e65. doi: 10.1161/CIRCULATIONAHA.104.496133.
27. Hou D, Youssef EA, Brinton TJ, Zhang P, Rogers P, Price ET, Yeung AC, Johnstone BH, Yock PG, March KL. Radiolabeled cell distribution after intramyocardial, intracoronary, and interstitial retrograde coronary venous delivery: implications for current clinical trials. *Circulation*. 2005;112:I150–I156. doi: 10.1161/CIRCULATIONAHA.104.526749.
28. Zhang M, Methot D, Poppa V, Fujio Y, Walsh K, Murry CE. Cardiomyocyte grafting for cardiac repair: graft cell death and anti-death strategies. *J Mol Cell Cardiol*. 2001;33:907–921. doi: 10.1006/jmcc.2001.1367.
29. Iacobazzi D, Mangialardi G, Gubernator M, Hofner M, Wielscher M, Vierlinger K, Reni C, Oikawa A, Spinetti G, Vono R, Sangalli E, Montagnani M, Madeddu P. Increased antioxidant defense mechanism in human adventitia-derived progenitor cells is associated with therapeutic benefit in ischemia. *Antioxid Redox Signal*. 2014;21:1591–1604. doi: 10.1089/ars.2013.5404.
30. Hatzistergos KE, Quevedo H, Oskouei BN, et al. Bone marrow mesenchymal stem cells stimulate cardiac stem cell proliferation and differentiation. *Circ Res*. 2010;107:913–922. doi: 10.1161/CIRCRESAHA.110.222703.
31. Gnecchi M, He H, Noiseux N, Liang OD, Zhang L, Morello F, Mu H, Melo LG, Pratt RE, Ingwall JS, Dzau VJ. Evidence supporting paracrine hypothesis for Akt-modified mesenchymal stem cell-mediated cardiac protection and functional improvement. *FASEB J*. 2006;20:661–669. doi: 10.1096/fj.05-5211com.
32. Timmers L, Lim SK, Arslan F, Armstrong JS, Hoefer IE, Doevendans PA, Piek JJ, El Oakley RM, Choo A, Lee CN, Pasterkamp G, de Kleijn DP. Reduction of myocardial infarct size by human mesenchymal stem cell conditioned medium. *Stem Cell Res*. 2007;1:129–137. doi: 10.1016/j.scr.2008.02.002.
33. Anand S, Majeti BK, Acevedo LM, Murphy EA, Mukthavaram R, Scheppke L, Huang M, Shields DJ, Lindquist JN, Lapinski PE, King PD, Weis SM, Cheresh DA. MicroRNA-132-mediated loss of p120RasGAP activates the endothelium to facilitate pathological angiogenesis. *Nat Med*. 2010;16:909–914. doi: 10.1038/nm.2186.
34. Connelly KA, Advani A, Zhang Y, Advani SL, Kabir G, Abadeh A, Desjardins JF, Mitchell M, Thai K and Gilbert RE. DPP-4 inhibition improves cardiac function in experimental myocardial infarction: Role of SDF-1 alpha. *Journal of diabetes*. 2015.
35. Wang X, Hu Q, Nakamura Y, Lee J, Zhang G, From AH, Zhang J. The role of the sca-1+/CD31- cardiac progenitor cell population in postinfarction left ventricular remodeling. *Stem Cells*. 2006;24:1779–1788. doi: 10.1634/stemcells.2005-0386.
36. Leri A, Anversa P. Stem cells and myocardial regeneration: cooperation wins over competition. *Circulation*. 2013;127:165–168. doi: 10.1161/CIRCULATIONAHA.112.153973.
37. Askari AT, Unzek S, Popovic ZB, Goldman CK, Forudi F, Kiedrowski M, Rovner A, Ellis SG, Thomas JD, DiCorleto PE, Topol EJ, Penn MS. Effect of stromal-cell-derived factor 1 on stem-cell homing and tissue regeneration in ischaemic cardiomyopathy. *Lancet*. 2003;362:697–703. doi: 10.1016/S0140-6736(03)14232-8.
38. Yamaguchi J, Kusano KF, Masuo O, Kawamoto A, Silver M, Murasawa S, Bosch-Marce M, Masuda H, Losordo DW, Isner JM, Asahara T. Stromal cell-derived factor-1 effects on ex vivo expanded endothelial progenitor cell recruitment for ischemic neovascularization. *Circulation*. 2003;107:1322–1328.
39. Zhang M, Mal N, Kiedrowski M, Chacko M, Askari AT, Popovic ZB, Koc ON, Penn MS. SDF-1 expression by mesenchymal stem cells results in trophic support of cardiac myocytes after myocardial infarction. *FASEB J*. 2007;21:3197–3207. doi: 10.1096/fj.06-6558com.
40. Elmadbouh I, Haider HKh, Jiang S, Idris NM, Lu G, Ashraf M. Ex vivo delivered stromal cell-derived factor-1alpha promotes stem cell homing and induces angiomyogenesis in the infarcted myocardium. *J Mol Cell Cardiol*. 2007;42:792–803. doi: 10.1016/j.yjmcc.2007.02.001.
41. Tang YL, Zhu W, Cheng M, Chen L, Zhang J, Sun T, Kishore R, Phillips MI, Losordo DW, Qin G. Hypoxic preconditioning enhances the benefit of cardiac progenitor cell therapy for treatment of myocardial infarction by inducing CXCR4 expression. *Circ Res*. 2009;104:1209–1216. doi: 10.1161/CIRCRESAHA.109.197723.
42. Unzek S, Zhang M, Mal N, Mills WR, Laurita KR, Penn MS. SDF-1 recruits cardiac stem cell-like cells that depolarize in vivo. *Cell Transplant*. 2007;16:879–886.
43. Bartunek J, Sherman W, Vanderheyden M, Fernandez-Aviles F, Wijns W, Terzic A. Delivery of biologics in cardiovascular regenerative medicine. *Clin Pharmacol Ther*. 2009;85:548–552. doi: 10.1038/clpt.2008.295.

Novelty and Significance

What Is Known?

- Preliminary evidence supports the feasibility and efficacy of cell therapy with autologous cardiac stem cells (CSCs) in patients with myocardial infarction (MI).
- Intramyocardial injection of human saphenous vein–derived pericytes (SVPs) supports reparative angiogenesis in a mouse model of acute MI, thereby promoting recovery of left ventricular function.
- Cell therapy with a combination of CSCs and bone marrow–derived mesenchymal stromal cells exerts additive effects in reducing the infarct size and improving the recovery of cardiac function in a swine model of cardiac ischemia–reperfusion.

What New Information Does This Article Contribute?

- Combined delivery of CSCs and SVPs in a mouse model of MI additively leads to a reduction in infarct size and an increase in arteriogenesis.
- CSCs and SVPs contribute to myocardial repair via complementary paracrine mechanisms; CSC promote cardiomyogenesis and SVPs vasculogenesis.
- In comparison with single cultures, cocultures of human CSCs and SVPs result in an increase in the release of the cardioprotective stromal cell–derived factor-1α (SDF-1α), likely because of the downregulation of dipeptidyl peptidase-4 (an stromal cell–derived factor-1–degrading enzyme) in CSCs.

Despite several clinical trials, an optimal stem cell–based strategy for the treatment of the failing heart has remained elusive. Hence, combinations of cells with complementary features may provide synergistic effects improving therapeutic outcomes. Starting from this consideration, we tested the effects of simultaneous injection of human CSCs and SVPs in a mouse model of acute MI. We selected these 2 cell populations because CSCs can differentiate in cardiomyocytes and vascular cells, and as we have demonstrated previously, SVPs support reparative angiogenesis in the infarcted heart, thereby promoting the recovery of left ventricular function. We found that in a murine model of MI, CSCs and SVPs act in a complementary fashion, promoting cardiomyogenesis and vasculogenesis, respectively. Importantly, when the cells were delivered together, we observed a reduction of infarct size and an augmentation of arteriogenesis. These findings reinforce the concept that combined treatments using cells with complementary potential may improve the efficacy of stem cell therapy in patients with MI.

SUPPLEMENTAL MATERIAL

LIST OF ABBREVIATIONS

ANG1 - Angiopoietin-1
ANG2 - Angiopoietin-2
CSCs - cardiac stem cells
DAPI - 4',6-diamidino-2-phenylindole
EdU - 5-ethynyl-2'-deoxyuridine
i.p. - intraperitoneal injection
MI - myocardial infarction
O.N. - over night, incubation of 16hrs at 4°C
PBS - phosphate buffered saline
PFA - paraformaldehyde
RT - room temperature
SDF-1 - stromal cells-derived factor 1
SVPs - saphenous vein derived pericytes
UCM - unconditioned medium

EXPANDED METHODS

Ethics

Experiments involving live animals were performed in accordance with the Guide for the Care and Use of Laboratory Animals published by the US National Institutes of Health (NIH Publication No. 85-23, revised 1996) and with the approval of the British Home Office and the University of Bristol. Studies on human cells complied with the ethical principles stated in the 'Declaration of Helsinki'. The use of human CSCs and SVPs was regulated by approvals from the Independent Ethics Committee of the University Hospital of Udine and South West-Bristol Central Research Ethics Committee. Informed written consent was obtained from patients.

Cell isolation and culture

CSCs: Discarded atrial specimens, weighing 3 to 6 g, were collected from hearts of healthy donors at the time of transplantation at the Cardiac Surgery Unit of the University Hospital of Udine (Italy). CSCs were isolated as described in[1]. Briefly, biopsies were collected in basic dissociation buffer (BDB)[1] containing penicillin and streptomycin. Myocardial tissue was carefully dissected from adipose tissue, endocardium and pericardium using sterile tweezers and scalpel, and then washed in BDB and digested for 5-10 minutes with 0.04% Collagenase type II (Sigma-Aldrich, Dorset, UK) in BDB. Tissue aggregates were eliminated by passing the cell suspension through a 40µm cell strainer. Finally, cells were plated in human MesenCult proliferation medium (STEMCELL Technologies, Manchester, UK) with the addition of 1X penicillin and streptomycin (Life Technologies, Paisley, UK). Starting from the second passage, cells were cultured in MAPCs medium (prepared as in[1]) on plates coated with human fibronectin (10µg/mL) (Sigma-Aldrich, Dorset, UK).

SVPs: Discarded saphenous vein specimens were collected from patients undergoing CABG surgery as previously described[2,3]. In brief, veins, collected in phosphate buffered saline (PBS) (Life Technologies, Paisley, UK) containing 1X penicillin and streptomycin (Life Technologies, Paisley, UK), were carefully dissected from surrounding tissues using a sterile scalpel and then thoroughly washed in excess PBS, containing antibiotics. Veins were then manually minced with a

scalpel before being incubated for 3-4 hours with 3.7mg/mL Liberase 2 (Roche, Basel, Switzerland), at 37°C in rotating tubes. The remaining aggregates were eliminated by passing the cell suspension through 30µm cell strainer. Cells were then incubated with anti-CD31 conjugated beads (Miltenyi, Bergisch Gladbach, Germany) for 30min at 4°C and passed through a magnetic column, following the manufacturer's instructions. This allowed efficient removal of mature endothelial cells. After depletion of CD31 positive cells, remaining cells were further incubated with anti-CD34 beads (Miltenyi, Bergisch Gladbach, Germany) for 30min at 4°C and then processed to obtain purified CD34 positive cells. Sorted cells were cultured on plates coated with Fibronectin (10µg/mL) and gelatin (0.1%) (both from Sigma-Aldrich, Dorset, UK) in the presence of growth medium, EGM2 +2% FBS (Lonza, Gloucestershire, UK).
All experiments were performed with CSCs and SVPs at passage 5-6.

Flow cytometry (FACS) analysis

SVPs and CSCs were stained for surface antigen expression using the following fluorochrome-conjugated antibodies: anti-CD90, anti-CD34, anti-CD31 (BD biosciences, Oxford, UK), anti-CD45 (Milteny, Bergisch Gladbach, Germany), anti-CD105 (Invitrogen, Paisley, UK), anti-CD44 (eBioscience, Hatfield, UK). After cell detachment, incubation was performed for 20 min at room temperature (RT), in the dark. The c-Kit antigen required a different procedure as it was an unconjugated antibody. After the first incubation with the anti-c-Kit antibody (Dako, 30 minutes at 37°C), cells were washed in PBS and incubated with a labelled secondary antibody for 20 minutes at 37°C.
After staining, cells were washed in PBS and fluorescence was analyzed using a FACS Canto II flow cytometer and FACS Diva software (both BD Biosciences, Oxford, UK). To control for specificity, isotype matched antibodies were employed as negative controls.

Cell characterization by immunofluorescence

For characterization, CSCs and SVPs were seeded at a density of 5,000 cells/cm^2 on 24-wells plate coverslips, fixed with 4% buffered paraformaldehyde (PFA) (Sigma-Aldrich, Dorset, UK) in PBS for 20min at RT and incubated with antibodies as specified in the table. For staining with c-Kit antibody, cells were fixed with PFA for 10 min at RT. Blocking was performed with 10% Goat Serum (GS) in PBS, for 30 mins at RT.
For detection of intracellular antigens, cells were permeabilized for 10 min at RT with 0.1% (v/v) Triton X100 (Sigma-Aldrich, Dorset, UK) diluted in PBS, before to proceed with antibody staining.
The table lists the antibody dilutions, incubation times (O.N.=overnight, 16hrs at 4°C) and temperatures employed. Incubations with primary and secondary antibodies were carried out in humid chambers. Nuclei were recognized by 4',6-diamidino-2-phenylindole (DAPI) staining. Cells were analyzed at a 400X magnification. Adobe Photoshop software was utilized to compose and overlay the images (Adobe).

Marker	**Permeabiliza-tion**	**Primary antibody**	**Secondary antibody**
Oct-4	yes	Abcam, 1:400, ON 4°C	Invitrogen, A488 Goat α-Rabbit, 1:200, 1h RT
Sox-2	yes	Millipore, 1:100, ON 4°C	Invitrogen, A488 Goat α-Rabbit, 1:200, 1h RT
Nanog	yes	Abcam, 1:100, ON 4°C	Invitrogen, A488 Goat α-Mouse, 1:200, 1h RT
c-Kit	no	Dako, 1:40, 2hrs 37°C	Invitrogen, A488 Goat α-Rabbit, 1:200, 1h RT
PDGFRβ	no	Santa Cruz, 1:50, ON 4°C	Invitrogen, A488 Goat α-Rabbit, 1:200, 1h RT
NG2	yes	Millipore, 1:100, ON 4°C	Invitrogen, A488 Goat α-Rabbit, 1:200, 1h RT

Differentiation assay toward the 3 cardiovascular lineages

To test the differentiative potential of CSCs and SVPs toward the 3 cardiovascular lineages (cardiomyocytes, endothelial cells and vascular smooth muscle cells), 3 cell lines of each type were seeded in differentiation medium at a density of 5,000 cells/cm^2, let to become confluent with media exchange every 3 days, for 14-21 days. The following differentiation methods and media were used:

- *endothelial differentiation*: CFU-Hill Liquid Medium Kit from STEMCELL Technologies, Manchester, UK, or a medium enriched with human VEGF (vascular endothelial growth factor, PeproTech EC Ltd, London, UK) as described in (Cesselli et al., 2013)[1];
- *cardiomyocyte differentiation*: 2 different methods were employed. The first is based on the culture of cells with a medium containing ascorbic acid (Sigma-Aldrich, Dorset, UK), 10ng/mL human bFGF (basic fibroblast growth factor), 10ng/mL VEGF and 10ng/mL IGF-1 (insulin-like growth factor 1) (all from PeproTech EC Ltd, London, UK), as described in (Cesselli et al., 2013)[1]; the second one is characterized by an initial 3-day long phase of demethylation by 5 μM 5-aza-2'-deoxycytidine (Sigma-Aldrich, Dorset, UK) and the following culture of cells with a medium containing ascorbic acid and 1ng/mL human TGF-β1 (transforming growth factor beta 1) (PeproTech EC Ltd, London, UK), as described in (Smits et al., 2009)[4];
- *smooth muscle cells differentiation*: differentiation medium added with 20ng/mL of human platelet-derived growth factor-BB (PDGF-BB, PeproTech EC Ltd, London, UK), as in (Cesselli et al., 2011)[5].

Cells were fixed with 4% PFA (Sigma-Aldrich, Dorset, UK) for 20 min at RT, permeabilized with 0.1% TritonX100 (Sigma-Aldrich, Dorset, UK) in PBS for 10min at RT when required, and stained with antibodies, in humid chambers in the dark, as illustrated in the table. Nuclei were recognized by DAPI staining. Cells were analyzed at a 400X magnification. Adobe Photoshop software was utilized to compose and overlay the images (Adobe).

Marker	Permeabi-lization	Primary antibody	Secondary antibody
CD31	no	Dako, 1:100, 2hrs 37°C	Invitrogen, A488 Goat α-Rabbit, 1:200, 1h RT
α-SMA	yes	Dako, 1:50, 2hrs 37°C	Invitrogen, A488 Goat α-Rabbit, 1:200, 1h RT
α-SA	yes	Sigma, 1:500, 1hr RT	Invitrogen, A555 Goat α-Mouse, 1:200, 1h RT
Connexin43	yes	Santa Cruz, 1:40, 2hrs 37°C	Invitrogen, A488 Goat α-Rabbit, 1:200, 1h RT
MHC	yes	Abcam, 1:100 ON 4°C	Invitrogen, A488 Goat α-Rabbit, 1:200, 1h RT

RealTime PCR analysis of SVPs after cardiomyocyte differentiation

To test the ability of SVPs to differentiate toward the cardiomyocyte lineage, total RNA was collected from n=3 lines of SVPs in basal culture conditions and after differentiation obtained with both the protocols described (see above).

RNA was extracted using Qiagen MiRNeasy kit (Life Technologies, Paisley, UK). The expression of the cardiac markers Tbx5, Connexin43, cardiac troponin T (CNNI3), cardiac myosin heavy chain (Myh7), Islet1, NKX2.5 and RyR2 were evaluated by reverse transcription using the High Capacity RNA-to-cDNA kit (Life Technologies, Paisley, UK) followed by quantitative PCR-based amplification using TaqMan probes (Life Technologies, Paisley, UK). The expression of UBC was employed as housekeeping gene to normalize the expression levels. Quantitative PCR was performed on a LightCycler480 Real-Time PCR system (Roche Technologies, Basel, Switzerland). Quantitative PCR parameters for cycling were as follows: 50° C incubation for 2 min, 95° C for 10 min, 40 cycles of PCR at 95° C for 15 s, and 65° C for 1 min. All reactions were performed in a 10 μl reaction volume in triplicate. The mRNA expression level was determined using the $2^{-\Delta Ct}$

method.[6] Values of gene expression are expressed as fold-change of differentiated cells with respect to basal cells.

Labelling of cells with long term trackers

For selected *in vivo* and *in vitro* experiments, CSCs and SVPs were stained respectively with the long term cell trackers VyBrant diO and VyBrant diL (Molecular Probes, Life Technologies, Paisley, UK). Briefly, diO and diL were diluted 1:1000 in PBS and incubated with confluent cells (adherent to the culture plate) for 5 min at 37°C and then on ice for further 15 min, in the dark. Cells were then washed with PBS and used for experiments.

Mouse model of myocardial infarction and cell transplantation

Two independent *in vivo* experiments were performed to test the short (14 days) and long (42 days) follow-up after myocardial infarction (MI) and cell transplantation.

MI was induced in 8 week-old female SCID Beige mice (Charles River) by permanent ligation of the left anterior descending coronary artery (LAD) as described in our earlier studies[7-9]. In brief, with mice under anesthesia (2,2,2 tribromo ethanol, 0.3gm/kg, i.p.) and artificial ventilation, the chest cavity was opened and, after careful dissection of the pericardium, LAD was permanently ligated using a 7-0 silk suture. This was followed by injection of either SVPs (300,000 cells, n=9 cell lines) (n=11 and 6 animals, for the short and long follow-up respectively) or CSCs (300,000 cells, n=9 cell lines) (n=12 and 7 animals) alone or in combination (300,000 cells for each type, n=9 cell lines for each type (n=12 and 7 animals)) at 3 different sites along the infarct border zone with final volume of 5µL at each site. Cells were resuspended in PBS for injection and were all at a passage 5 or 6 of culture. Vehicle animals (n=14 and 7 for 14 days and 42 days follow-up, respectively) received PBS injection in the similar manner. Sham-operated mice (n=6), in which the chest was opened without MI induction or any therapy, were used as control.

For the short-term recovery experiment (14 days post-MI), a selected number of animals were transplanted with cells pre-labelled with the long term cell trackers VyBrant-DiI (for SVPs) and VyBrant-diO (for CSCs) (see above) to allow the recognition of human cells in the mouse heart. Another group of animals received unlabeled CSCs and SVPs and i.p. injection of 360µg EdU (resuspended in 100µL of sterile PBS, both from Life Technologies, Paisley, UK) every 2 days, for all the recovery period, in order to assess the cumulative vasculogenesis and cardiomyogenesis during the 14 days post-MI period.

We previously determined the optimal dose of SVPs and CSCs for injection in the animal heart, in order to reach positive results at the functional outcome[10,11]. We decided to inject the double amount of cells in the combined SVP+CSC therapy in order to obtain the maximum beneficial effects given by each cell population.

Animals were allowed to recover with aseptic precautions and received analgesic medication (Buprenorphine, 0.1mg/kg s.c.) to reduce post-operative pain.

Echocardiography and hemodynamic measurements

Measurements of dimensional and functional parameters were performed before and at 14 and 42 days after MI using a high-frequency, high resolution echocardiography system (Vevo 770, Visual Sonics, Toronto, Canada). Briefly, mice were anesthetized using tribromo-ethanol and transferred to an imaging stage equipped with a warming pad for controlled maintenance of mouse body temperature at 37°C and a built-in electrocardiography system for continuous heart rate (HR) and respiratory rate monitoring. The thickness of the left ventricle (LV) was measured at the level of the papillary muscles in parasternal short axis at end-systole and end-diastole. LV

ejection fraction (LVEF) and fractional shortening (LVFS) were determined as described by De Simone *et al*.[8,9,12] Following the final echocardiography measurement on day 14 and 42 post-MI, under anesthesia, intraventricular pressure measurement was done using a high-fidelity 1.4F transducer tipped catheter (Millar Instruments, Houston, TX, USA) inserted into the left ventricle through right carotid artery. The position of transducer into the heart was confirmed by the rapid deflection of the diastolic pressure wave without any change in systolic pressure. After 5 min stabilization, baseline data were collected, including the HR, Peak LV systolic pressure (LVESP), LV end-diastolic pressure (LVEDP), and maximal rates of LV pressure rise (dP/dt_{max}) and fall (dP/dt_{min}).[8,9,13] To calculate pressure volume relationship, the recording from Millar catheter was synchronized with echocardiography measurements as per manufacturer instructions.[7-9]

Samples processing for histology

After completion of hemodynamic measurements, hearts were stopped in diastole by intramyocardial injection of 0.1M cadmium chloride. Hearts were then washed free of blood by retrograde perfusion with PBS-2% EDTA solution, followed by fixation with freshly prepared ice-cold 4% w/v PFA (Sigma-Aldrich, Dorset, UK) in PBS, (1) shortly in perfusion and (2) for 24 hours at 4°C after explantation of the organ. Then, hearts were washed with PBS and cryoprotected overnight at 4°C in PBS containing 10% w/v sucrose (Sigma-Aldrich, Dorset, UK). Tissues were then cut transversally in the middle in order to obtain 2 separate portions: the apex/middle and middle/base of the heart, and were embedded in Tissue-Tek compound (OCT) and frozen at -80°C.

For a selected number of samples, the atria and the right ventricle were separated from the left ventricle, and the mass of this latter has been measured before cryoprotection with Sucrose and cryopreservation in OCT.

Immunohistochemistry on ventricular sections

Immunohistochemistry analysis was performed on left ventricular cryosections (8µm thick) post-fixed with 4% PFA (Sigma-Aldrich, Dorset, UK) in PBS, for 20 min at RT, or with ice-cold Acetone, for 10 min at -20°C, followed by permeabilization with 0.1% Triton X-100 in PBS, for 10 min at RT. Slides used for histology were pre-treated with VECTABOND reagent (Vector Laboratories, UK).

Assessment of human cell engraftment and in vivo differentiation

For the detection of non-labelled human cells in the mouse hearts at 14 and 42 days post-MI, *n*=3-4 sections were incubated with a mouse monoclonal anti-Human Nuclei antibody (Millipore, UK, 1:100, O.N. 4°C), followed by goat-anti mouse secondary antibody conjugated with Alexa Fluor 568 (Invitrogen, UK, 1:200, 1h RT). A human myocardial sample was employed as positive control for the labelling efficiency of the antibody. To assess the cardiomyocyte differentiation, sections were incubated with a mouse monoclonal anti-α-sarcomeric actin (Sigma-Aldrich, Dorset, UK, 1:200, 1h 37°C) followed by goat-anti mouse IgM secondary antibody conjugated with Alexa Fluor 647 (Invitrogen, UK, 1:200, 1h RT). For endothelial markers, sections were incubated either with a sheep anti-human CD34 (DAKO, UK, 1:100, ON 4°C) followed by a donkey anti-sheep secondary antibody conjugated with Alexa Fluor 488 (Invitrogen, UK, 1:200, 1h RT), or with biotinylated Isolectin B4 (Invitrogen, UK, 1:200, ON 4°C) followed by streptavidin Alexa Fluor 488 (Invitrogen, UK, 1:200, 1h at RT). Nuclei were recognized by DAPI staining.

In 14 days post-MI samples, when pre-labelled, injected SVPs were identified by the Vybrant Dil red fluorescence, while injected CSCs were recognized by the Vybrant DiO green fluorescence.

Spectral Analysis for Human Nuclei immunolabelling

To assess the specificity of the Human Nuclei immunolabelling protocol, spectral analysis was performed with a TCS-SP2 confocal microscope (Leica, Wetzlar, Germany) using the lambda acquisition mode, as in[5]. Lens and corresponding numerical aperture were 63X and 1.4, respectively. 8μm SVP- and CSC-transplanted heart cryosections, cut along the infarcted left ventricle, were labelled with a mouse anti-Human Nuclei antibody followed by AlexaFluor 568 goat anti-mouse secondary antibody (see above for the labelling protocol). Nuclei were stained with DAPI. The emission signal for AlexaFluor 568 was excited at a wavelength of 513 nm with an argon laser, and the fluorescence emitted from the tissue was recorded over the interval from 515 to 750 nm. A series of 30 images were acquired at a 7.9 nm intervals.

This operation was followed by both the calculation of the emission spectra and by the spectral dye separation, to selectively distinguish the specific Dye emission (corresponding to Human Nuclei) from the aspecific one (corresponding to lipofuscines). Sampling consisted of at least 15 Human Nuclei-positive cells and 15 Lipofuscines, randomly collected from SVP- and CSC-injected hearts. Additionally, 15 fluorescent signals corresponding to the background autofluorescence of the tissue, present in the same samples, were used as control, to discriminate background autofluorescence from specific labeling. Finally, graphs plotting mean pixel intensity and the emission wavelength of the lambda stack were generated.

Vascular density profiling

For capillary density, n=3 5μm thick LV cryosections were incubated with biotinylated Isolectin B4 (Invitrogen, UK, 1:200, ON 4°C, in a humidified chamber), followed by streptavidin Alexa Fluor 488 (Invitrogen, UK, 1:200, 1h at RT). For arteriole density, the same sections were probed with anti-mouse α-smooth muscle cell actin antibody conjugated with Cy3 (Sigma chemicals, UK, 1:400, 1h at RT). Capillaries and arterioles were calculated in 10 fields (at a X400 magnification) in the peri-infarct myocardium, and the final data expressed as the number of capillaries or arterioles per square millimeter. Arterioles were also categorized according to their luminal size.[7,14] The analysis was performed using the free software ImageJ (http://imagej.nih.gov/ij/). Adobe Photoshop software was utilized to compose and overlay the images (Adobe).

Cardiomyocyte proliferation and apoptosis

For analysis of proliferation, *n*=2 sections were incubated with rabbit polyclonal Ki67 antibody (Abcam, UK, 1:500, O.N. 4°C), followed by goat-anti rabbit secondary antibody conjugated with Alexa Fluor 549 (Invitrogen, UK, 1:400, 1h 37°C), and mouse monoclonal α-sarcomeric actin (Sigma, 1:200, 1h 37°C) followed by goat-anti mouse secondary antibody conjugated with Alexa Fluor 488 (Invitrogen, UK, 1:500, 1h 37°C). Nuclei were recognized by DAPI staining. The data were expressed as fraction of $Ki67^{pos}$ myocyte nuclei in the border zone.

Cardiomyocyte apoptosis was quantified by the terminal deoxynucleotidyl-transferase (TdT)-mediated dUTP nick-end labeling (TUNEL) technique (in situ cell death detection kit Fluorescein, Apoptag, Millipore, Germany). Following the treatment of n=2 slides with proteinase K (Sigma, 15μg/ml, 10min at RT), the TUNEL assay was performed according to the manufacturer's instructions. Finally sections were stained with DAPI to recognize nuclei. The data were expressed as fraction of TdT^{pos} myocytes nuclei in peri-infarct zone. Sections were analysed at a 400X magnification. Adobe Photoshop software was utilized to compose and overlay the images (Adobe).

Identification of cardiac stem cell pool in myocardium

For identification of the cardiac stem cell pool in the myocardium, n=3 sections were incubated with a goat polyclonal antibody specifically reactive with the mouse c-Kit antigen (R&D, USA, 1:100, 2h at 37°C), followed by donkey anti-goat Alexa Fluor 555 antibody (Invitrogen, USA, 1:800); mouse monoclonal mast cell tryptase (Abcam, USA, 1:400, 2h at 37°C), followed by donkey anti-mouse Alexa Fluor 488 antibody (Invitrogen, USA, 1:800); and mouse monoclonal α-sarcomeric actin (Sigma Chemicals, Italy, 1:200, 1h at 37°C), followed by donkey anti-mouse DyLight 649 antibody (Invitrogen, USA, 1:400). Nuclei were recognized by DAPI staining. The data were expressed as the density of cells in peri-infarct zone. Sections were analysed at a 630X magnification. Adobe Photoshop software was utilized to compose and overlay the images (Adobe).

Assessment of cumulative vasculogenesis and myocardial proliferation

EdU-treated hearts were used for this analysis. n=3 sections were first processed using the Click-IT EdU 488 or 555 Imaging kit (Life Technologies, Paisley, UK) to reveal EdU incorporation, according to the manufacturer's instructions. Sections were then stained for alpha-sarcomeric actin, Isolectin-B4 or alpha-SMA, as already indicated above. Nuclei were recognized by DAPI staining. Sections were analysed at a 400X magnification. Data were expressed as fraction of EdU^{pos} cardiomyocyte nuclei or as the number of capillaries or arterioles including endothelial/smooth muscle cells EdU-positive nuclei per square millimeter, in the border zone. Arterioles were also categorized according to their luminal size.

Assessment of infarct size and myocardial fibrosis

Infarct size was evaluated in n=3 not consecutive sections cut at different levels along the infarcted left ventricle, by Azan Mallory staining as in[7]. Two different methods (area and length-based measurements) were applied in 14 and 42 days post-MI samples, as previously explained in[15]. Infarct size is expressed as the percentage of the left ventricle sectional area occupied by the fibrotic scar.

Myocardial interstitial fibrosis was analyzed in n=3 sections by Azan Mallory staining. Fifteen fields were randomly evaluated in the spared myocardium at a 400X magnification. Data are expressed as the percentage of fibrotic area.

Adobe Photoshop software was utilized to compose and adjust the contrast of the images (Adobe). Analysis was performed using the free software ImageJ (http://imagej.nih.gov/ij/).

Assessment of cardiomyocyte hypertrophy and nuclear density

Cardiomyocyte cross sectional area (CSA) and cardiomyocyte nuclear density were evaluated in n=3 not consecutive sections cut at different levels along the infarcted left ventricle. Sections were incubated with an Alexa Fluor 488-conjugated anti-Wheat Germ Agglutinin antibody (Invitrogen, UK, 1:100, 30 min RT) and with a mouse monoclonal anti-α-sarcomeric actin antibody (Sigma, UK, 1:200, 1h 37°C) followed by goat-anti mouse IgM secondary antibody conjugated with Tritc (Invitrogen, UK, 1:200, 1h RT). Nuclei were recognized by DAPI staining. Sections were analysed at a 400X magnification. Analysis were performed using the free software ImageJ (http://imagej.nih.gov/ij/). For each sample, CSA was measured in 100 cardiomyocytes in which the nucleus was centrally located within the cell, in both the border peri-infarct zone and in the remote zone. The average regional cross-sectional area and regional myocyte nuclear density per mm^2 were calculated.

Collection of cell supernatants for secretome and in vitro studies

Confluent CSCs or SVPs or CSCs+SVPs were incubated with serum-free EGM-2 medium (Lonza, Gloucestershire, UK) for 48 hrs, in normoxic (20% O_2) or hypoxic (2% O_2) culture conditions. 1mL of medium was added to the cells for every 10cm^2 of the plate surface. The same number of CSCs and SVPs were initially seeded in the single and combined cultures, so that in these latter the number of cells was two-fold respect to the single cell cultures and followed the ratio of 1:1 as for the cell transplantation in the mouse hearts.

To mimic the *in vivo* ischemia situation, all the conditioned media employed for *in vitro* experiments (with cardiomyocytes, mouse CSCs and HUVECs) were collected incubating cells in hypoxia. Cell supernatants were collected, centrifuged at 1,000xg for 10 minutes at 4°C and stored at -80°C until use.

Analysis of cell secretome by ELISA

Human VEGF (vascular endothelial growth factor), bFGF (basic fibroblasts growth factor), HGF (hepatocyte growth factor), SCF (stem cell factor), ANG1 (Angiopoietin-1), ANG2 (Angiopoietin-2), SDF-1 (stromal cells-derived factor 1) and CD26/DPP-4 released in cell supernatants in normoxic and/or hypoxic culture (collected as described above) were dosed using DuoSet Development System by R&D or CD26/DPP-4 ELISA kit from Sigma-Aldrich, following manufacturer's instructions. The amounts of all factors were expressed normalizing the data for the number of the cells at the end of the collection time and for the time of incubation.

Evaluation of transcriptional regulation of secreted factors in CSCs and SVPs

To evaluate if the release of SDF-1, ANG1, ANG2 and DPP-4 by co-cultures of CSCs and SVPs is regulated at the transcriptional level, confluent cultures of CSCs (n=3-4) and SVPs (n=3-5) were incubated for 6 hours with EGM-2 medium conditioned by the other cell type (n=3 CSCs or n=3 SVPs) for 48hrs in normoxia or hypoxia. Unconditioned medium (UCM) was used as control.

At the end of the incubation period, total RNA was collected and extracted using Qiagen MiRNeasy kit (Life Technologies, Paisley, UK). The expression of SDF-1, Angiopoietins and DPP-4 genes were evaluated by reverse transcription using the High Capacity RNA-to-cDNA kit (Life Technologies, Paisley, UK) followed by quantitative PCR-based amplification using TaqMan probes (Life Technologies, Paisley, UK). The expression of UBC was employed as housekeeping gene to normalize the expression levels. Quantitative PCR was performed on a LightCycler480 Real-Time PCR system (Roche Technologies). Quantitative PCR parameters for cycling were as follows: 50° C incubation for 2 min, 95° C for 10 min, 40 cycles of PCR at 95° C for 15 s, and 65° C for 1 min. All reactions were performed in a 10 µl reaction volume in triplicate. The mRNA expression level was determined using the $2^{-\Delta Ct}$ method.

MicroRNA-132 expression in conditioned media

The release of miR-132 was investigated in CSCs (n=3), SVPs (n=3) and co-coltures of CSCs+SVPs (n=3), in normoxic and hypoxic culture conditions. For samples collection, 200µL of medium was added to 1mL of QIAzol lysis reagent (Qiagen, Venlo, Netherlands). RNA was extracted using Qiagen MiRNeasy kit (Qiagen, Venlo, Netherlands). Extracted total RNA was reverse-transcribed using specific primers provided with the Taqman miRNA assay and MicroRNA Reverse Transcription Kit (Life Technologies, Paisley, UK). A microRNA synthetic spike was used to assess microRNA isolation efficiency and act as an internal control. *Caenorhabditis elegans* miRNA-39-3p (Life Technologies, Paisley, UK) was added to the conditioned media prior to RNA extraction. The synthetic spike and target genes were *Caenorhabditis elegans* miRNA-39-3p and MicroRNA -132-3p.

Quantitative PCR was performed on a LightCycler480 Real-Time PCR system (Roche Technologies, Basel, Switzerland). Quantitative PCR parameters for cycling were as follows: 50° C incubation for 2 min, 95° C for 10 min, 40 cycles of PCR at 95° C for 15 s, and 60° C for 1 min. All reactions were performed in a 10 µl reaction volume in triplicate. The mRNA expression level was determined using the $2^{-\Delta Ct}$ method. One-way ANOVA and Dunnet's post-test multiple comparison test using mean values and standard error were used to compare results. These were performed on all the fold change means in all groups assessed, allowing the significance of multiple means to be assessed.

Co-culture assays: in vitro interaction between SVPs and CSCs.

1- EdU proliferation assay

CSCs (n=3) and diL-labelled SVPs (n=3) were seeded in single or co-cultures in EGM-2 medium added of 2% FBS (both from Lonza, Gloucestershire, UK), on coated coverslips in 24-well plates. For co-cultures, the same number of CSCs and SVPs in single cultures was seeded, so that the final number of cells was two-fold respect to the single cell cultures, and followed the ratio 1:1 between cells. After incubation for 20 hrs in presence of EdU in the culture medium, cells were fixed with buffered 4% PFA (Sigma-Aldrich, Dorset, UK) in PBS for 15min at RT and stained following manufacturer's instructions (Click-iT® EdU Imaging Kit, from Invitrogen, Paisley, UK). Nuclei were stained with DAPI. Experiments were performed in duplicate. Cells were analysed at a 400X magnification and the percentage of EdU+ cells was determined for each cell population.

2- Tunel apoptosis assay with CSCs and SVPs in contact

CSCs (n=3) and diL-labelled SVPs (n=3) were seeded in single or co-cultures in FBS free EGM-2 medium (both from Lonza, Gloucestershire, UK), on coated coverslips in 24-well plates. After 48 hrs of starvation, cells were fixed with 1% PFA (Sigma-Aldrich, Dorset, UK) in PBS for 10 min at RT and TUNEL assay was performed following manufacturer's instructions (in situ cell death detection kit Fluorescein, Apoptag, Millipore, Germany). A negative and positive (treatment of cells with Dnase) control were included. Nuclei were stained with DAPI. Experiments were performed in duplicate. Cells were analyzed at a 400X magnification and the percentage of TdT+ cells was determined for each cell population.

3- Tunel apoptosis assay with CSCs and SVPs kept separated by a membrane

n=3 CSCs and n=3 SVPs lines were co-cultured (in all the possible combinations of CSCs+SVPs) using 24MW plates transwell membrane inserts with 0.4µm pores (CORNING, UK), that allow to grow different cells together but without contacts between cells. SVPs and CSCs cultured alone were used as control. 20,000 cells of one cell type were seeded on the bottom of the well and 20,000 cells of the other cell type were added on the membrane. Cells were incubated with serum free EGM-2 for 48hrs. At the end of the starvation period, cells seeded on the bottom of the wells were fixed with 1% PFA (Sigma-Aldrich, Dorset, UK) in PBS for 10 min at RT and TUNEL assay was performed according to the manufacturer's instructions (in situ cell death detection kit Fluorescein, Apoptag, Millipore, Germany). A negative and positive (treatment of cells with Dnase) control were included. Nuclei were stained with DAPI. Experiments were performed in duplicate. Cells were analyzed at a 200X magnification and the percentage of TdT+ cells was determined for each cell population.

Paracrine effects of CSCs and SVPs on isolated rat cardiomyocytes: apoptosis assay.

Cardiomyocytes were isolated from adult male rats. Animals were killed by stunning and cervical dislocation prior to dissection of the heart. Ventricular cardiomyocytes were isolated by the Langendorff method, using collagenase perfusion. At the end of the isolation procedure, Calcium was reintroduced gradually in the cell suspension to reach a concentration of 1.8 mM.

Cardiomyocytes were then plated at a density of 10,000 cells/cm^2 on murine laminin (5μg/cm^2, Sigma-Aldrich, Dorset, UK) coated 96-well plates, in a myocyte culture medium composed as follows: medium 199, 2g/L BSA, 2% FBS, 2mM Carnitine, 5mM Creatine, 5mM Taurine, 1mM Butanedione and antibiotics (all from Sigma-Aldrich, Dorset, UK), pH=7.35, and incubated for 1hr at 37°C, 5% CO2 to allow attachment to culture dish. Then culture medium was replaced with fresh one and cells were incubated for 4 more hours.

Cardiomyocytes were then subjected to Simulated Ischemia (SI) for 1 hr by replacing the medium with an "ischemia buffer" composed as follows: 118 mM NaCl, 24 mM $NaHCO_3$, 1.0 mM NaH_2PO_4, 2.5 mM $CaCl_2$-$2H_2O$, 1.2 mM $MgCl_2$, 20 mM sodium DL- lactate, 16 mM KCl, 10 mM 2-deoxy-D-glucose (all from Sigma-Aldrich, Dorset, UK), pH=6.2, and incubating cells at 37°C, 1% O_2 and 5% CO_2. ReOxygenation (RO) was then accomplished incubating the cells for 17h at 37°C, 5%CO_2, in cardiomyocyte medium conditioned by CSCs (n=3), SVPs (n=3) or co-cultured SVPs+CSCs (n=3) and diluted 1:2 with fresh medium prior to incubation with cardiomyocytes. Unconditioned cardiomyocyte medium was employed as control. To validate the pro-apoptotic effect of the SI/RO protocol employed, control cardiomyocytes were also cultured in normoxic conditions (without SI/RO). At the end of the reoxygenation period, the activity of caspase 3/7 in cardiomyocytes was evaluated employing the Caspase-Glo 3/7 assay (Promega, United Kingdom), following manufacturer's instructions. Experiments were performed in quadruplicate. Caspase activity in treated cardiomyocytes is expressed as fold change of caspase activity in cells treated with UCM.

To test the purity of isolated cells, cardiomyocytes were washed with PBS and fixed with 4% PFA (Sigma-Aldrich, Dorset, UK), in PBS for 20 minutes at RT, permeabilized using 0,1% Triton-X100 in PBS (Sigma-Aldrich, Dorset, UK), 10 min at RT, and stained with an anti-alpha sarcomeric actinin antibody (Sigma, mouse monoclonal, 1:500 dilution, 1hr 37°C) followed by incubation with an Alexa555 goat-anti-mouse secondary antibody (Invitrogen, 1:200 dilution in PBS, 1hr at room temperature). Nuclei were stained with DAPI. Cells were analyzed at a X400 magnification.

Paracrine effects of CSCs and SVPs on isolated mouse cardiac Sca-1+ cells.

Sca-1$^+$ cells were isolated from n=5 CD1 mouse (Charles River) hearts using the Cardiac Stem Cells Isolation Kit (Millipore, Germany) following manufacturer's instructions. Cells were cultured and expanded in DMEM (Invitrogen, Paisley, UK) + 5% FBS (Life Technologies, Paisley, UK) until use.

To test the purity of isolated cells, these latter were seeded in 8-chamber slides coated with Fibronectin (10μg/mL) and gelatin (0.1%) (both from Sigma-Aldrich, Dorset, UK), cultured and fixed with 4% PFA (Sigma-Aldrich, Dorset, UK) in PBS for 20 minutes at RT; cells were stained with a Tritc-conjugated antibody against mouse Sca-1 (BD biosciences, Oxford, UK), 1:20 dilution, incubated for 1hr at 37°C. Nuclei were stained with DAPI. Cells were analyzed at a X400 magnification. Adobe Photoshop software was utilized to compose the images (Adobe).

BrdU proliferation assay

3,000 Sca-1+ cells were seeded in each well of a 96-well plate and incubated for 16 hrs with EGM-2 medium (Lonza, Gloucestershire, UK) conditioned by CSCs (n=3), SVPs (n=3) or co-cultured SVPs+CSCs (n=3) and additioned of 5% FBS (Lonza, Gloucestershire, UK) and BrdU (10μmol/L). Unconditioned EGM-2 was employed as control. After this period, the incorporation of BrdU by cells was measured using a BrdU assay kit from Roche Technologies, Basel, Switzerland, according to the manufacturer's instructions. Briefly, cells were fixed and made permeable with FixDenat solution for 20min, then incubated with monoclonal anti-BrdU peroxidase-conjugated antibody (anti-BrdU-POD) for 90min. Bound anti-BrdU-POD was detected by a substrate reaction, then quantified by an ELISA plate reader. Experiments were performed in triplicate. Proliferation in treated groups is expressed as fold change of proliferation in cells treated with UCM.

Caspase 3/7 apoptosis assay

3,000 Sca-1+ cells were seeded in each well of a 96-well plate and incubated for 48 hrs with FBS-free EGM-2 medium (Lonza, Gloucestershire, UK) conditioned by CSCs (n=3), SVPs (n=3) or co-cultured SVPs+CSCs (n=3). Unconditioned EGM-2 was employed as control. After this period, the activity of caspase 3/7 was evaluated employing the Caspase-Glo 3/7 assay (Promega, United Kingdom), following manufacturer's instructions. Experiments were performed in quadruplicate. Caspase activity in treated groups is expressed as fold change of caspase activity in cells treated with UCM.

Migration toward CSC and SVP conditioned medium

To test the capacity of CSC and SVP secretome to induce the migration of Sca-1+ CSCs, 40,000 mouse Sca-1+ CSCs were seeded in 24-well plates on a 6.5mm Transwell® with 5.0μm Pore Polycarbonate Membrane Insert (Corning, UK), in serum-free EGM-2 medium (Lonza, Gloucestershire, UK). In the bottom of the wells, 0.5 mL of CSCs (n=3), SVPs (n=3) or co-cultured SVPs+CSCs (n=3) conditioned medium was added, as a stimulus to induce Sca-1^+ CSC migration. Serum-free unconditioned EGM-2 was used as control. Cells were incubated for 8 hrs at 37°C. At the end of this period, the membrane inserts were washed with PBS, fixed with 4% PFA (Sigma-Aldrich, Dorset, UK) in PBS for 20 min at RT, stained with DAPI and mounted on a slide. Membranes were analysed with an epifluorescence microscope at a 200X magnification; 10 fields were randomly acquired and migrated cells counted. No cells were detectable in the lower chamber of the 24-well plate. Migrated cells were expressed as percentage of total cells. Experiments were performed in duplicates.

In vitro matrigel assay with HUVECs

The capacity of CSC, SVP and co-cultured CSC+SVP secretomes to induce the formation of an endothelial cell network of human umbilical vein endothelial cells (HUVECs, Cambrex/Lonza) was evaluated using an extracellular matrix (ECM) gel assay (BD Bioscience, Oxford, UK). 70 μL of matrigel was added into each well of an ice-cold 96-well plate and incubated for 30 minutes at 37°C. This was performed on ice. 8000 HUVECs at passage 5 were resuspended in 100 μL of conditioned medium from CSCs (n=5), SVPs (n=5) and CSCs+SVPs (n=5) previously diluted 1:1 with new fresh EGM-2 medium supplemented with 5% FBS (Lonza, Gloucestershire, UK). The cells were added on the top of the gelified matrigel (100 μL/well) and incubated for 6 hours at 37°C, 5% CO_2. Unconditioned EGM-2 was used as control.

The assay was performed in quadruplicate. Network formation was analyzed in an Axiovert microscope (Zeiss); an image for each well was acquired at a magnification of 50X. For quantification, the length of the networks was measured using the software ImageJ (http:// rsb.info.nih.gov/ij/) and the cumulative tube length (in mm) per field was calculated.

BrdU proliferation assay with HUVECs

1,500 HUVECs were seeded in each well of a 96-well plate and incubated for 40 hrs with EGM-2 medium (Lonza, Gloucestershire, UK) conditioned by CSCs (n=3), SVPs (n=3) or co-cultured SVPs+CSCs (n=3) and additioned of 5% FBS (Lonza, Gloucestershire, UK) and BrdU (10μmol/L). Unconditioned EGM-2 was employed as control. After this period, the incorporation of BrdU by cells was measured using a BrdU assay kit from Roche Technologies, Basel, Switzerland, according to the manufacturer's instructions. Briefly, cells were fixed and made permeable with FixDenat solution for 20min, then incubated with monoclonal anti-BrdU peroxidase-conjugated antibody (anti-BrdU-POD) for 90min. Bound anti-BrdU-POD was detected by a substrate reaction,

then quantified by an ELISA plate reader. Experiments were performed in triplicate. Proliferation in treated groups is expressed as fold change of proliferation in cells treated with UCM.

In vitro matrigel assay with SVPs and CSCs

The capacity of SVPs, CSCs and co-culture of SVP+CSC (n=4 for each cell type) to form tubular networks was evaluated using an extracellular matrix (ECM) gel assay (BD Bioscience, Oxford, UK). 70 μL of matrigel was added into each well of an ice-cold 96-well plate and incubated for 30 minutes at 37°C. This was performed on ice. 4,000 SVPs, 4,000 CSCs or 4,000 SVPs + 4,000 CSCs at passage 5 were resuspended in 100 μL of EGM-2 medium supplemented with 2% FBS (Lonza, Gloucestershire, UK). The cells were added on the top of the gelified matrigel (100 μL/well) and incubated for 5 hours at 37°C, 5% CO_2.

The assay was performed in triplicate. Network formation was analyzed in an Axiovert microscope (Zeiss); an image for each well was acquired at a magnification of 50X. For quantification, the length of the networks was measured using the software ImageJ and the cumulative tube length (in mm) per field was calculated.

Statistics

Results are expressed as mean±SEM. After the normality test, comparison of multiple groups was performed by 1 way ANOVA or Kruskal-Wallis test as appropriate, followed respectively by Bonferroni or Dunns post-test. Difference between two groups was analyzed using t-test (paired or unpaired as appropriate). A P value of <0.05 was considered statistically significant.

Analyses were conducted with GraphPad Prism software.

1. Cesselli D, D'Aurizio F, Marcon P, Bergamin N, Beltrami CA, Beltrami AP. Cardiac stem cell senescence. *Methods Mol Biol* 2013; **976**: 81-97.
2. Campagnolo P, Cesselli D, Al Haj Zen A, et al. Human adult vena saphena contains perivascular progenitor cells endowed with clonogenic and proangiogenic potential. *Circulation* 2010; **121**(15): 1735-45.
3. Katare R, Riu F, Mitchell K, et al. Transplantation of human pericyte progenitor cells improves the repair of infarcted heart through activation of an angiogenic program involving micro-RNA-132. *Circulation research* 2011; **109**(8): 894-906.
4. Smits AM, van Vliet P, Metz CH, et al. Human cardiomyocyte progenitor cells differentiate into functional mature cardiomyocytes: an in vitro model for studying human cardiac physiology and pathophysiology. *Nature protocols* 2009; **4**(2): 232-43.
5. Cesselli D, Beltrami AP, D'Aurizio F, et al. Effects of Age and Heart Failure on Human Cardiac Stem Cell Function. *Am J Pathol* 2011; **179**(1): 349-66.
6. Livak KJ, Schmittgen TD. Analysis of relative gene expression data using real-time quantitative PCR and the 2(-Delta Delta C(T)) Method. *Methods* 2001; **25**(4): 402-8.
7. Katare R, Caporali A, Emanueli C, Madeddu P. Benfotiamine improves functional recovery of the infarcted heart via activation of pro-survival G6PD/Akt signaling pathway and modulation of neurohormonal response. *Journal of molecular and cellular cardiology*; **49**(4): 625-38.
8. Meloni M, Caporali A, Graiani G, et al. Nerve growth factor promotes cardiac repair following myocardial infarction. *Circulation research*; **106**(7): 1275-84.
9. Katare R, Caporali A, Zentilin L, et al. Intravenous gene therapy with PIM-1 via a cardiotropic viral vector halts the progression of diabetic cardiomyopathy through promotion of prosurvival signaling. *Circulation research* 2010; **108**(10): 1238-51.
10. Katare R, Riu F, Mitchell K, et al. Transplantation of Human Pericyte Progenitor Cells Improves the Repair of Infarcted Heart Through Activation of an Angiogenic Program Involving Micro-RNA-132. *Circ Res* 2011; **109**(8): 894-906.
11. Avolio E, Gianfranceschi G, Cesselli D, et al. Ex vivo molecular rejuvenation improves the therapeutic activity of senescent human cardiac stem cells in a mouse model of myocardial infarction. *Stem Cells* 2014.
12. de Simone G, Wallerson DC, Volpe M, Devereux RB. Echocardiographic measurement of left ventricular mass and volume in normotensive and hypertensive rats. Necropsy validation. *Am J Hypertens* 1990; **3**(9): 688-96.
13. Spillmann F, Graiani G, Van Linthout S, et al. Regional and global protective effects of tissue kallikrein gene delivery to the peri-infarct myocardium. *Regenerative medicine* 2006; **1**(2): 235-54.
14. Stone OA, Richer C, Emanueli C, et al. Critical role of tissue kallikrein in vessel formation and maturation: implications for therapeutic revascularization. *Arteriosclerosis, thrombosis, and vascular biology* 2009; **29**(5): 657-64.
15. Takagawa J, Zhang Y, Wong ML, et al. Myocardial infarct size measurement in the mouse chronic infarction model: comparison of area- and length-based approaches. *Journal of applied physiology* 2007; **102**(6): 2104-11.

ONLINE SUPPLEMENTAL TABLES & FIGURES

ONLINE SUPPLEMENTARY TABLE

CELL LINES USED FOR IN VITRO EXPERIMENTS				
	Nr of patients	***Gender (M/F)***	***Age (yrs)****	***Pathology******
SVP	18	16/2	66 ± 4	CAD
CSC	10	6/4	54 ± 3	n.a.

CELL LINES USED FOR IN VIVO STUDIES				
	Nr of patients	***Gender (M/F)***	***Age (yrs)*,****	***Pathology******
SVP	9	8/1	57 ± 6	CAD
CSC	9	5/4	55 ± 3	n.a.

* Values are expressed as mean ± SEM

** T-test SVP vs CSC p=0.78

*** CAD, Coronary Artery Disease

n.a. not applicable

ONLINE FIGURE I

A

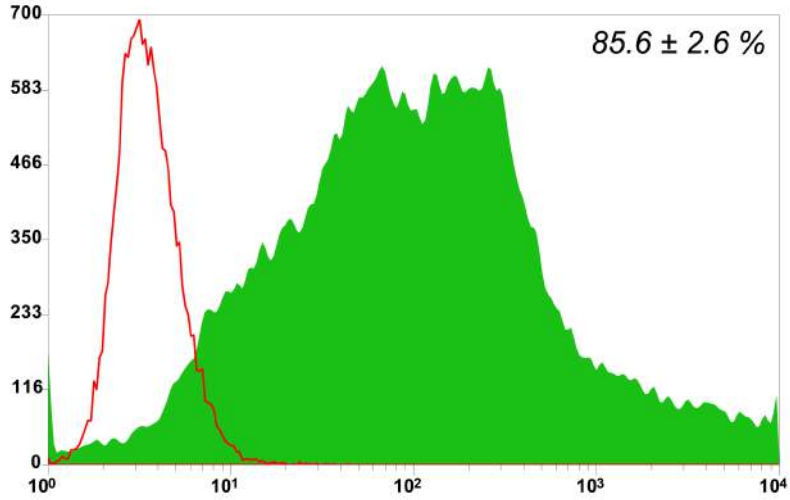

B

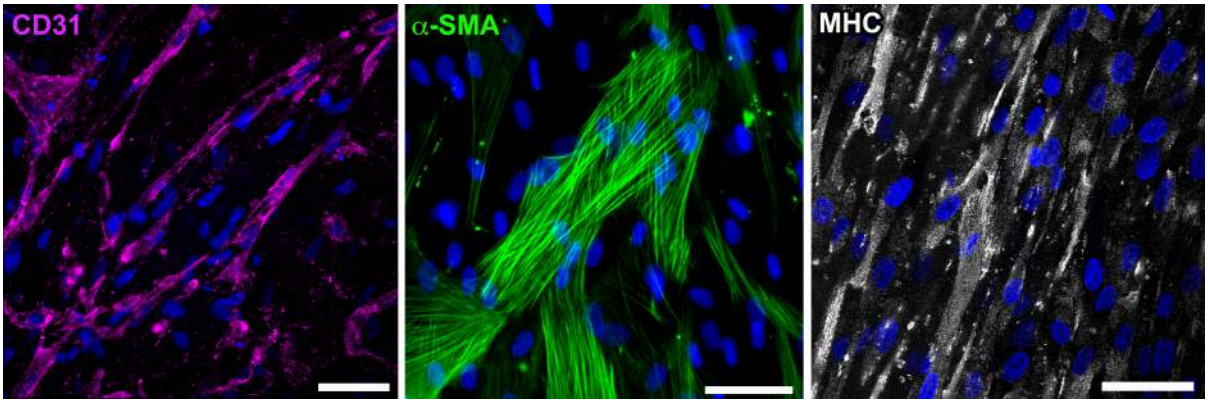

Online figure I. **CSCs characterization. (A) Flow cytometry analysis of c-Kit expression in CSC lines employed for in vitro and in vivo experiments.** Isotype control IgG staining profiles are shown by the red border line histograms, while specific antibody staining profiles are shown by full green histograms. Data are expressed as means±SEM **(**n=12). **(B) Immunofluorescence images showing the CSC plasticity toward the 3 cardiovascular lineages.** When cultured for 2-3 weeks in specific inductive media, CSCs are able to differentiate in endothelial cells expressing CD31, vascular smooth muscle cells positive for the contractile protein alpha-smooth muscle actin (α-SMA), and cardiomyocyte-like cells expressing the contractile filament MHC (myosin heavy chain). Nuclei are shown by the blue fluorescence of 4', 6-diamidino-2-phenylindole (DAPI). Scale bar: 50μm.

ONLINE FIGURE II

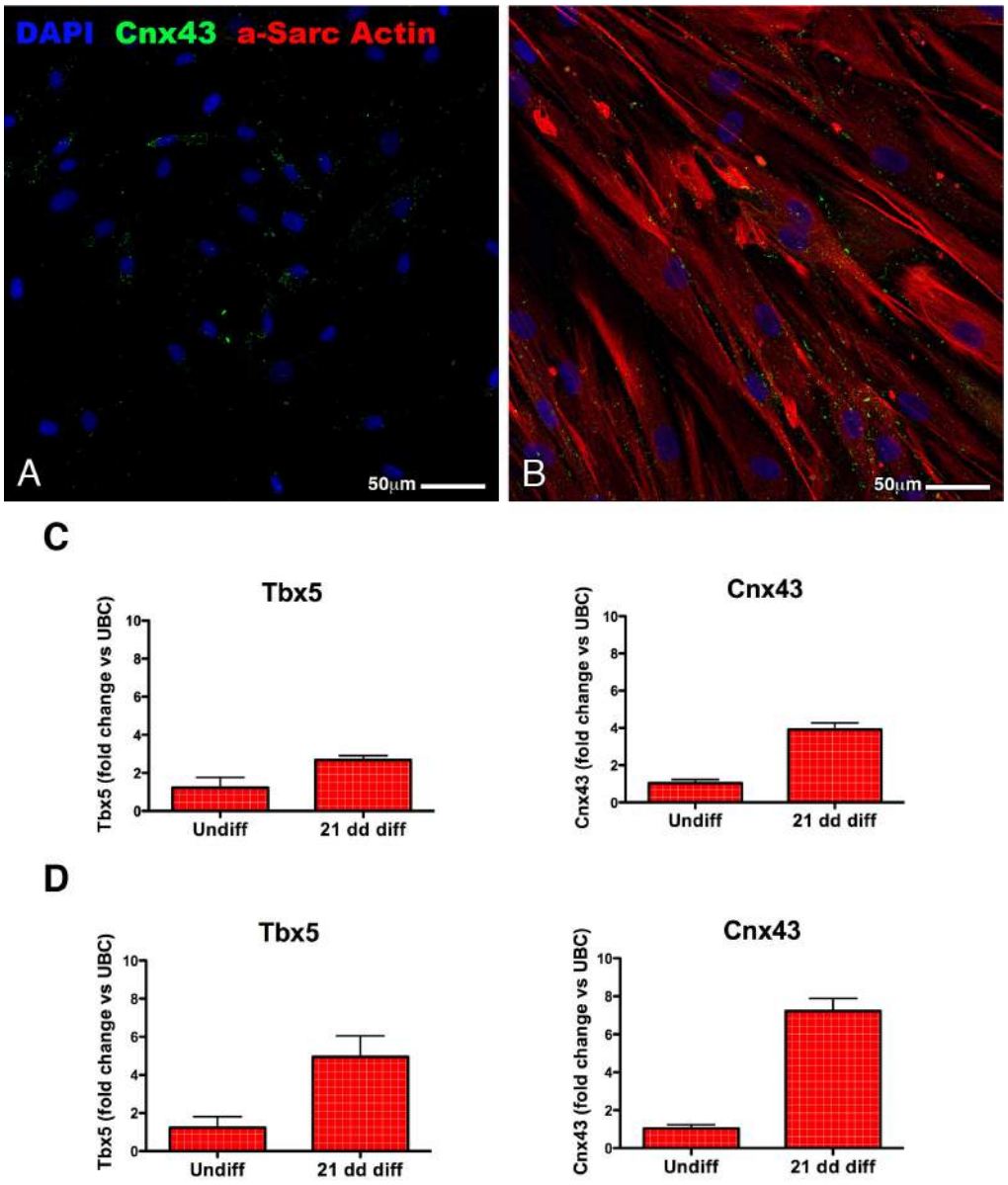

Online figure II. **Differentiation of SVPs toward the cardiomyocyte lineage**. At immunofluorescence analysis, undifferentiated SVPs express Connexin-43 (in green) but are negative for the cytoplasmic protein α-Sarcomeric Actin **(A)**, while after culture for 21 days with an inductive medium, cells express α-Sarcomeric Actin (red) **(B)**. Nuclei are shown by the blue fluorescence of 4', 6-diamidino-2-phenylindole (DAPI). Bar graphs show the results of qPCR analyses of Connexin-43 and Tbx5 mRNA levels in SVPs (n=3 biological replicates) before and after induction of cardiomyocyte differentiation using the protocols described in Beltrami et al., 2007 **(C)** and Smits et al., 2009 **(D)** (see methods). Data are presented as mean±SEM.

ONLINE FIGURE III

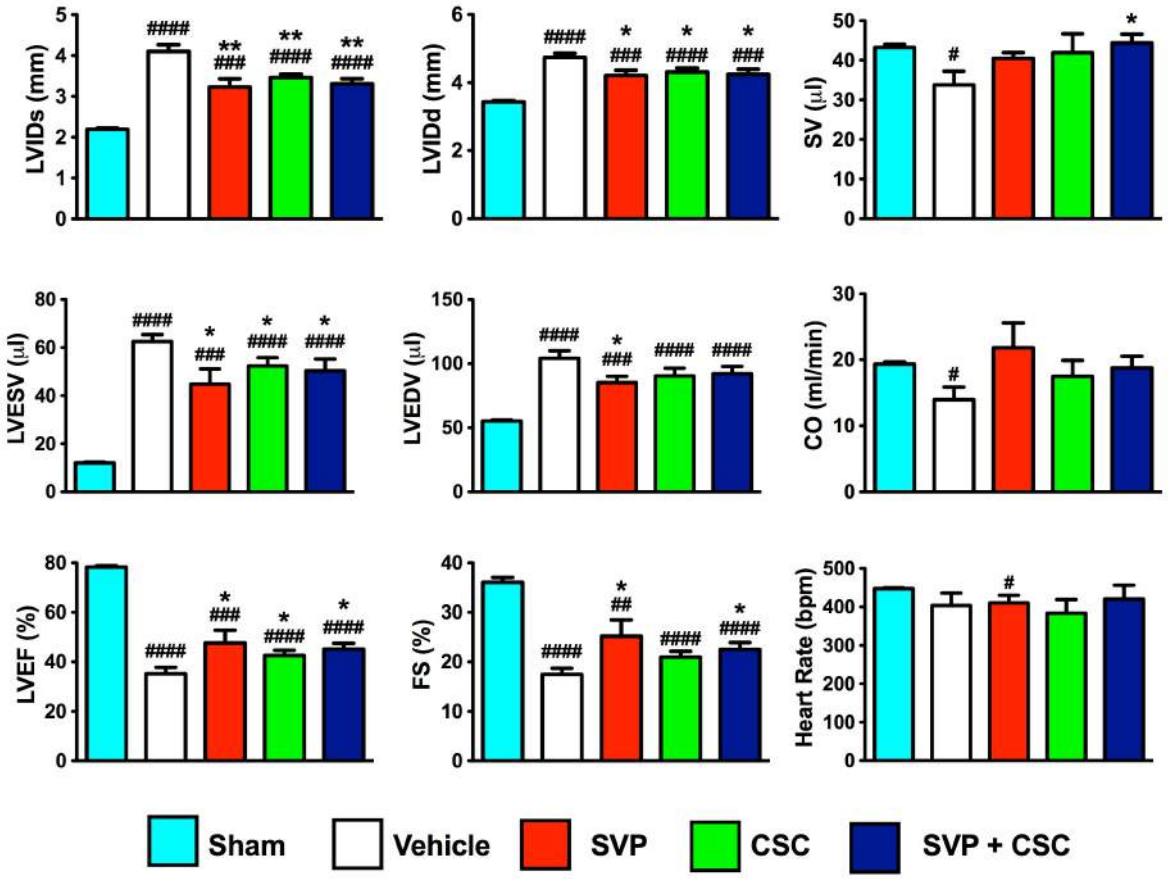

Online figure III. **Effect of single or combined cell therapy on echocardiographic and hemodynamic parameters 42 days post-myocardial infarction (MI).** SCID/Beige immunodeficient mice were intramyocardially injected with SVPs (300,000cells/heart), CSCs (300,000cells/heart), SVPs+CSCs (300,000cells of each type/heart) or Vehicle at the occasion of MI induction and measurements were performed 42 days thereafter. Sham operated mice were included as control. LVID, left ventricle internal diameter; LVESV, LV end-systolic volume; LVEDV, LV end-diastolic volume; SV, stroke volume; CO, cardiac output; LVEF, LV ejection fraction; FS, fractional shortening; LVAW, LV anterior wall; LVESP, LV end-systolic pressure; LVEDP, left ventricle end-diastolic pressure; s, systole; d, diastole. Data are presented as mean±SEM (n=6-7 mice per group). $^{\#}$p<0.05, $^{\#\#}$p<0.01, $^{\#\#\#}$p<0.001, $^{\#\#\#\#}$p<0.0001 vs. Sham; *p<0.05, **p<0.01 vs. Vehicle.

ONLINE FIGURE IV

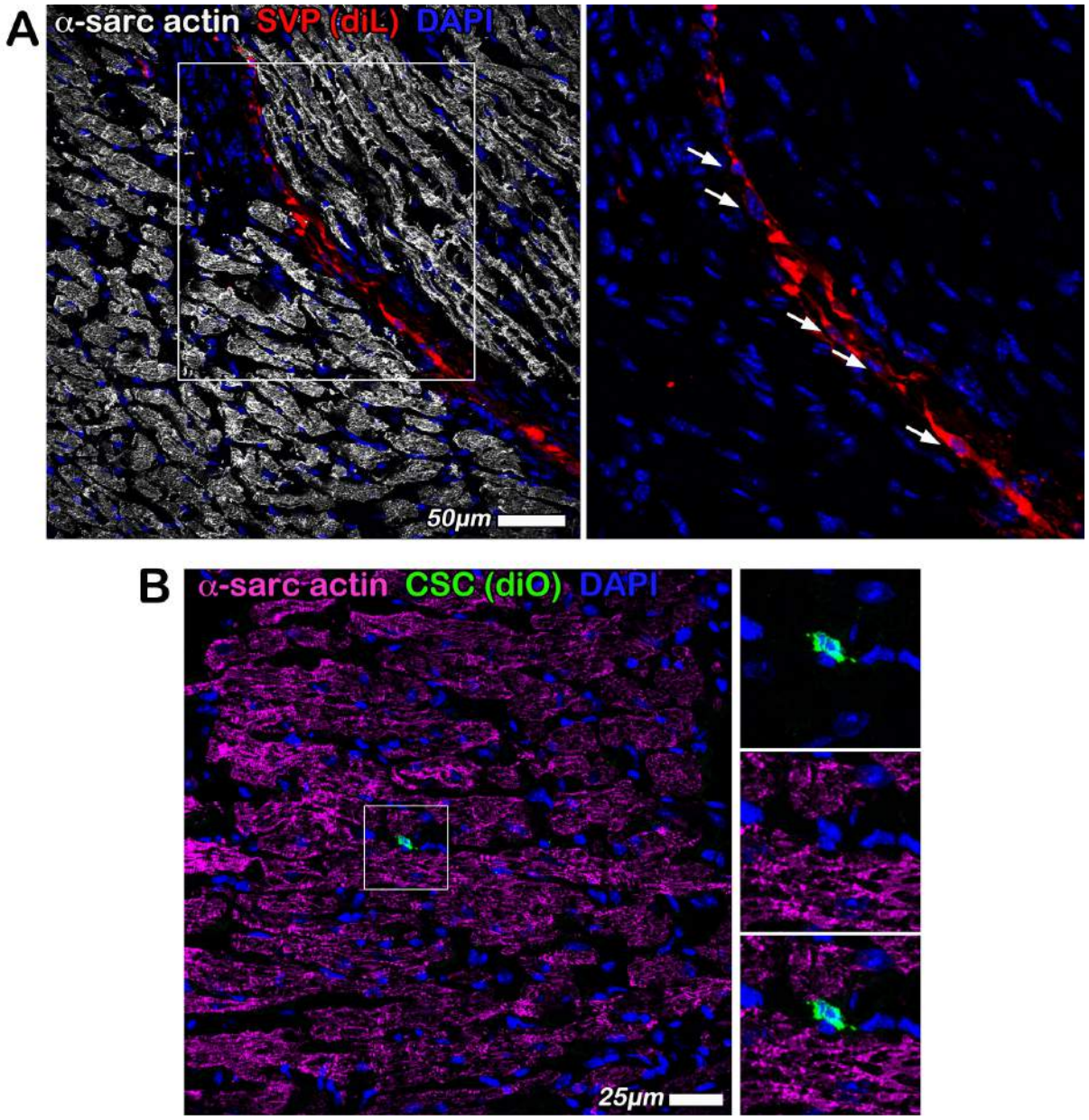

ONLINE FIGURE IV

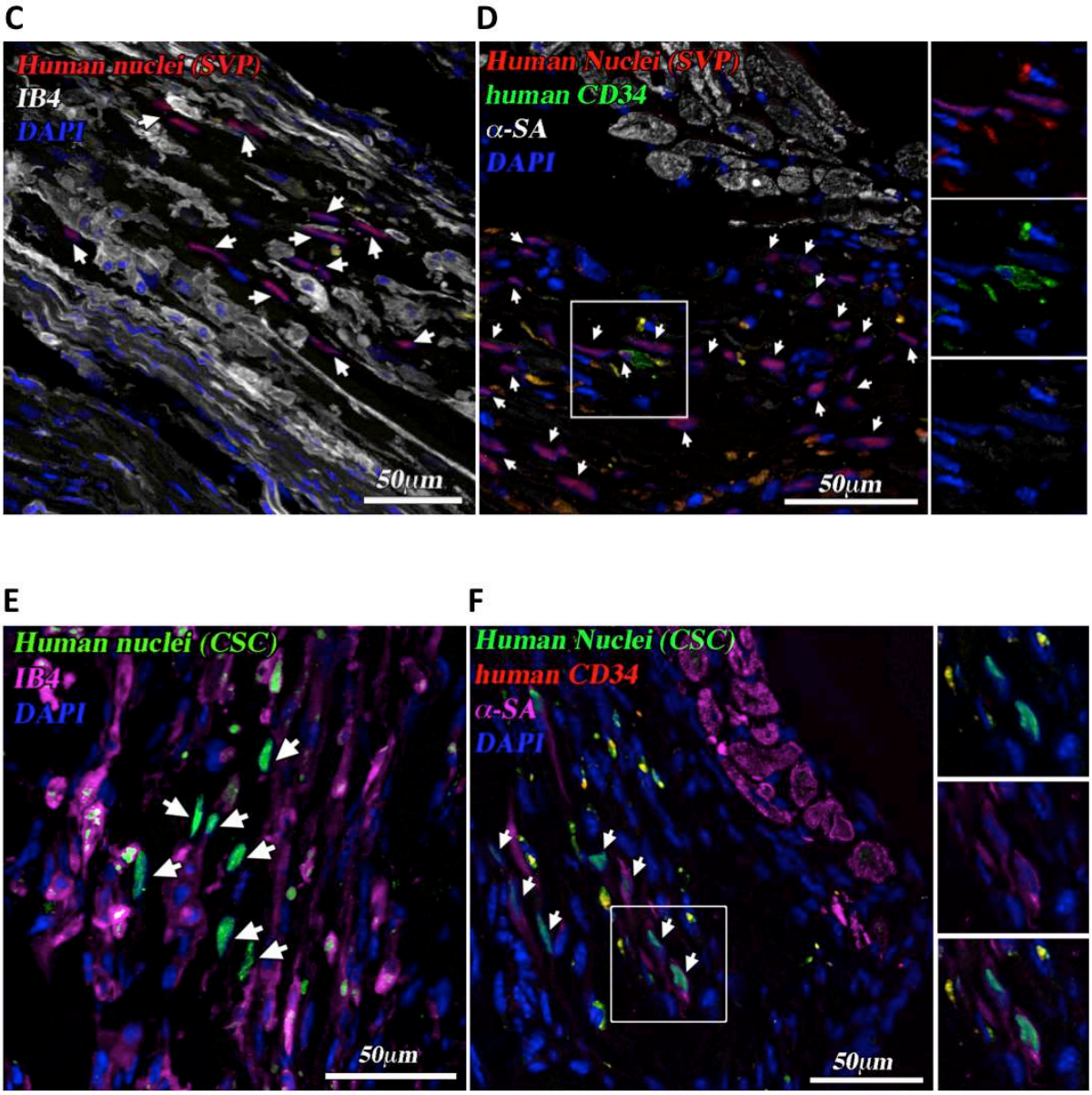

Online figure IV. **Engraftment and differentiation of CSCs and SVPs in the mouse heart at 14 days post-MI.** Confocal images showing human cells engraftment in the mouse heart. **(A):** SVPs showed with the red fluorescence of diL and **(B)**: CSCs showed with the green fluorescence of diO. α-Sarcomeric Actin labels cardiomyocyte cytoplasm and is showed in white in (A) and in magenta in (B). Nuclei (DAPI) are depicted in blue. **(C-F)** Human cells are recognised by fluorescent immunostaining with an anti-human nuclei antibody. SVPs nuclei, identified by white arrows, are depicted in red **(C&D),** while CSCs nuclei are shown in green **(E&F)**. The mouse endothelial marker Isolectin B4 is showed in white in **(C)** and in magenta in **(E)**, while the endothelial marker human CD34 is showed in green in **(D)** and in red in **(F).** α-Sarcomeric Actin, that labels cardiomyocyte cytoplasm, is depicted in white in **(D)** and in magenta in **(F)**. Nuclei (DAPI) are identified in blue fluorescence.

ONLINE FIGURE V

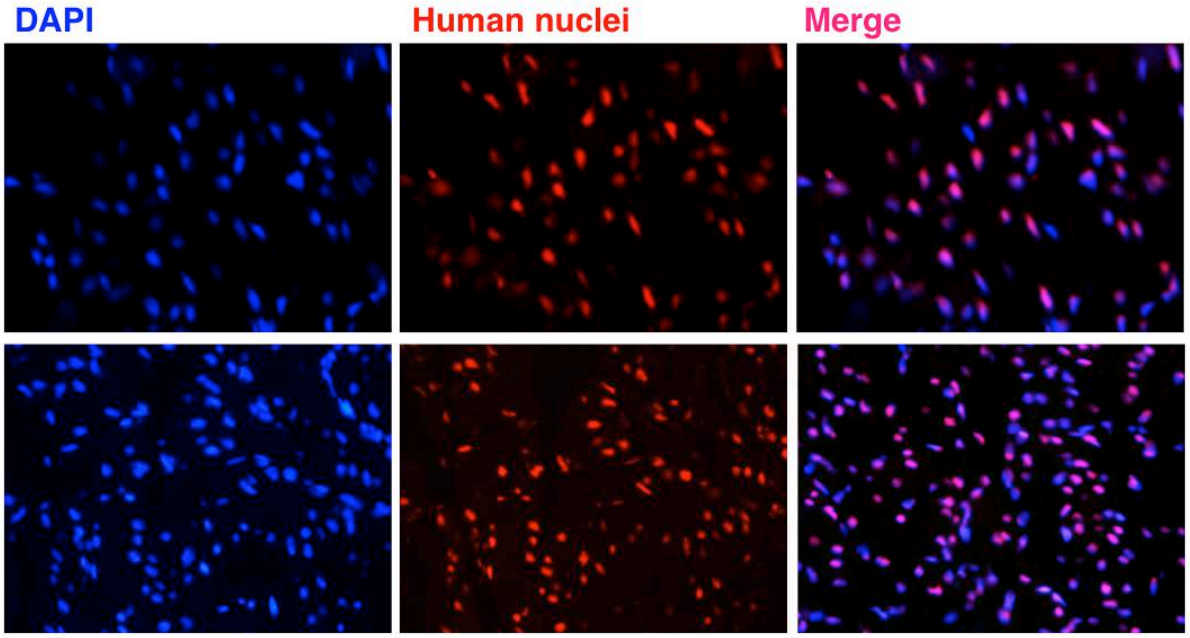

Online figure V. **Staining of the human heart with the anti-human nuclei antibody.** Positive control to verify the labelling efficiency of the antibody used for identification of human donor cells in mouse hearts. The labelling efficiency was of 96% (red fluorescence). Nuclei (DAPI) are identified in blue fluorescence. Magnification: 400X.

ONLINE FIGURE VI

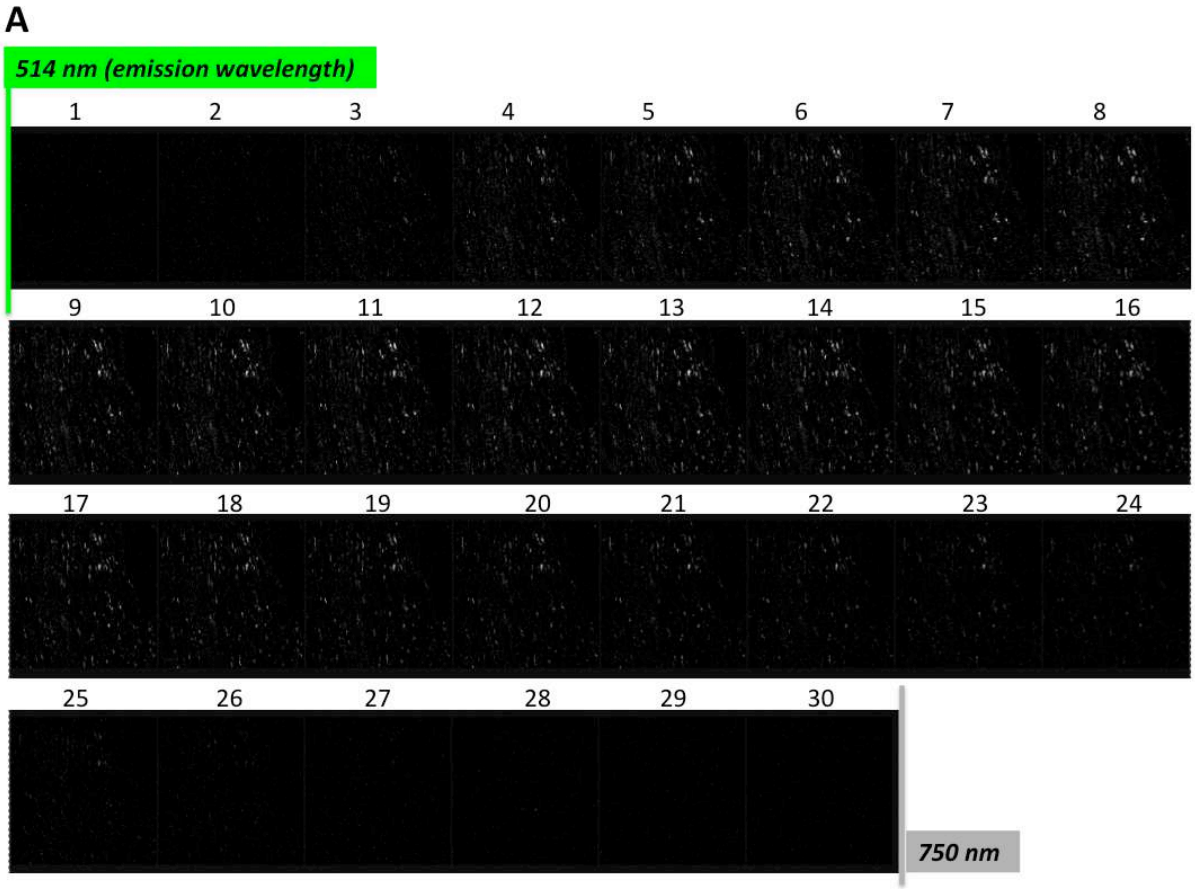

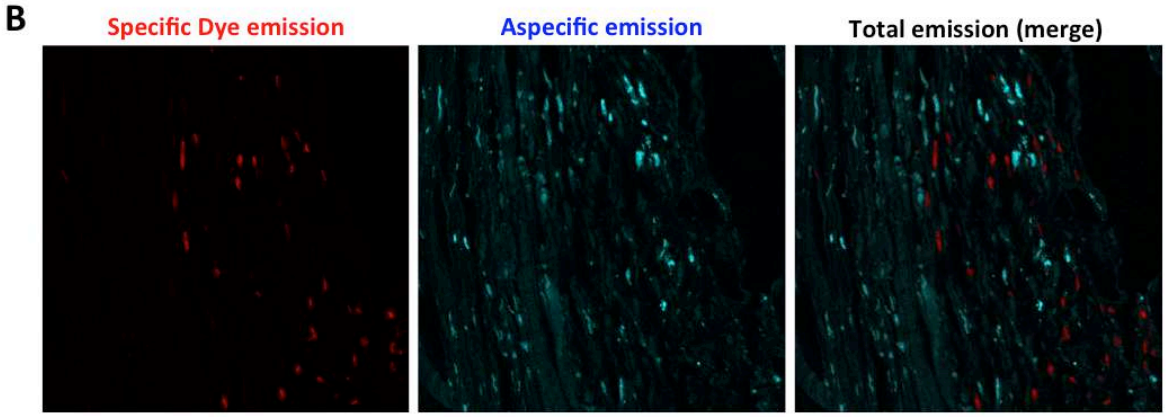

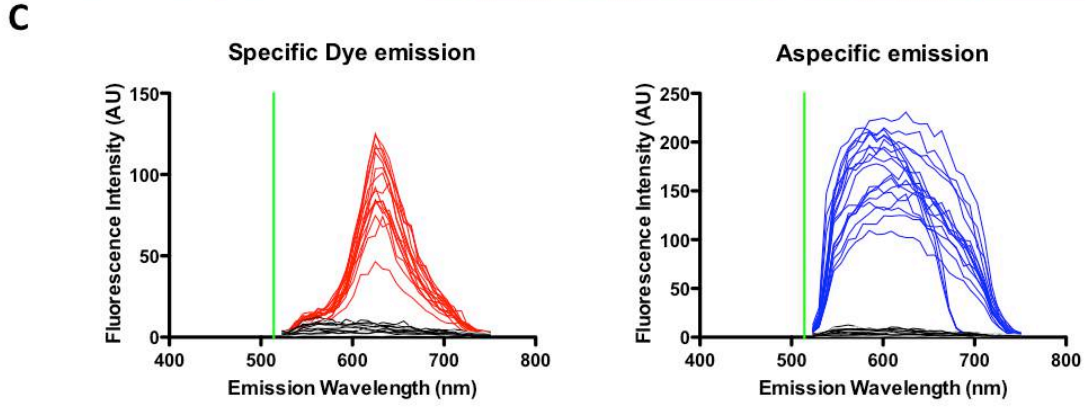

Online Figure VI: Validation of immunolabeling by spectral analysis of human-nuclei positivity in the mice hearts. 8μm sections of SVP- and CSC-transplanted hearts were stained with a mouse anti-Human Nuclei antibody followed by AlexaFluor 568 goat anti-mouse secondary antibody. **(A)** Representative confocal single channel Lambda-scan acquisition. Samples were excited at a wavelength of 513 nm and the fluorescence emitted from the tissue was recorded over the interval from 515 to 750 nm. A series of 30 images was acquired. The fluorescence recorded at the different wavelengths is shown in white. This operation was followed by both the calculation of the emission spectra and by the spectral dye separation. **(B)** Representative pictures in which the specific Dye emission (in red, corresponding to Human Nuclei) was separated from the unspecific emission (in blue) performing a spectral dye separation. Unspecific emission is attributable to the presence of lipofuscines (in yellow in Suppl. Fig 4D&F). **(C)** Graphs illustrate that the specific emission spectra of the AlexaFluor 568 Dye (on the left, red curves) are clearly distinct from the unspecific emission spectra of lipofuscines (on the right, blue curves), and from the background autofluorescence of the tissue, showed with black curves, thus confirming the accuracy of the analysis indicating the presence of human cells in the recipient hearts. The green bar corresponds to the excitation wavelength. A minimum of n=15 emission spectra have been reported in each case, randomly collected from CSC- and SVP-injected hearts.

ONLINE FIGURE VII

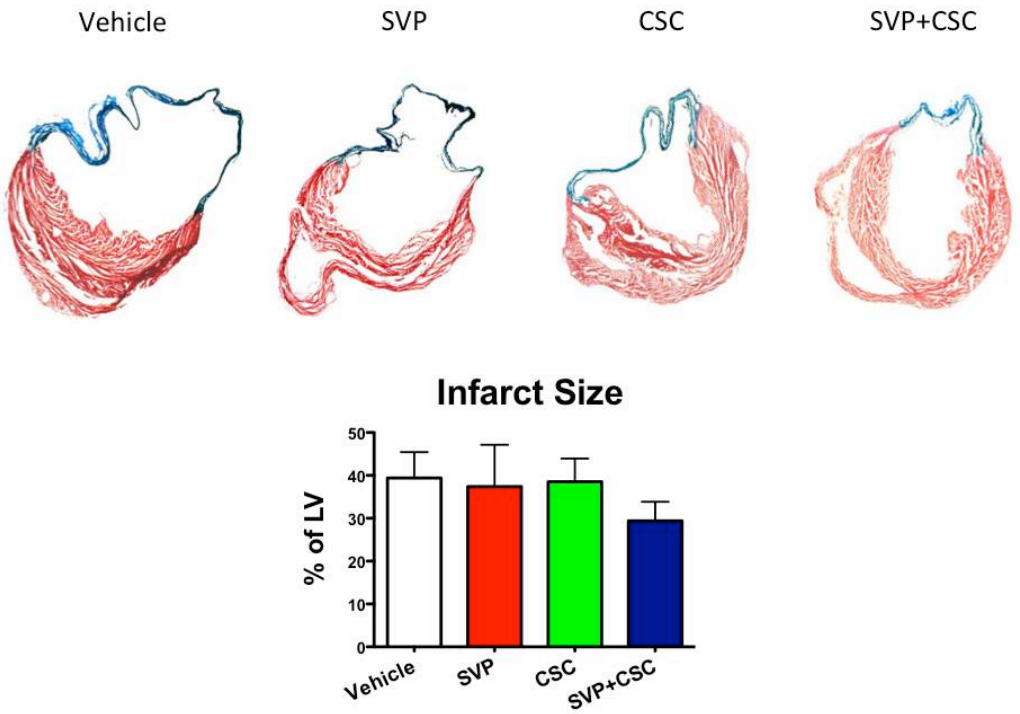

***Online figure VII. E*valuation of infarct size in mice 42 days post-MI and cell therapy.** Representative images of Azan Mallory staining in ventricular sections; collagen fibres are stained in blue (12.5X magnification). The bar graphs summarize quantitative data of the percentage of the LV area occupied by the scar. Data are presented as mean±SEM (n=5-7 mice per group).

ONLINE FIGURE VIII

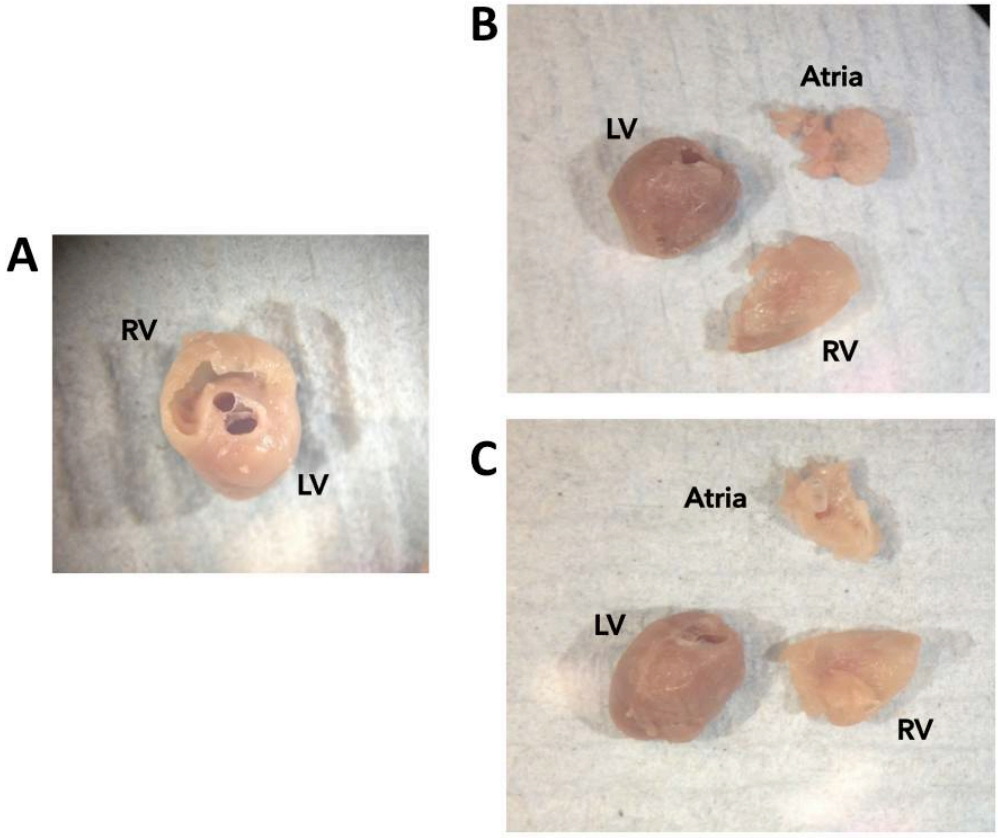

Online figure VIII. **Separation of the left ventricle (LV) in mice hearts 14 days post-MI.** For a selected number of mice (n=6 per each MI-group and n=3 Sham) the LV was separated from the rest of the heart for histological morphometric evaluation. After the initial removal of the atria from the ventricles **(A)**, the right ventricle (RV) was further separated from the LV **(B&C)**.

ONLINE FIGURE IX

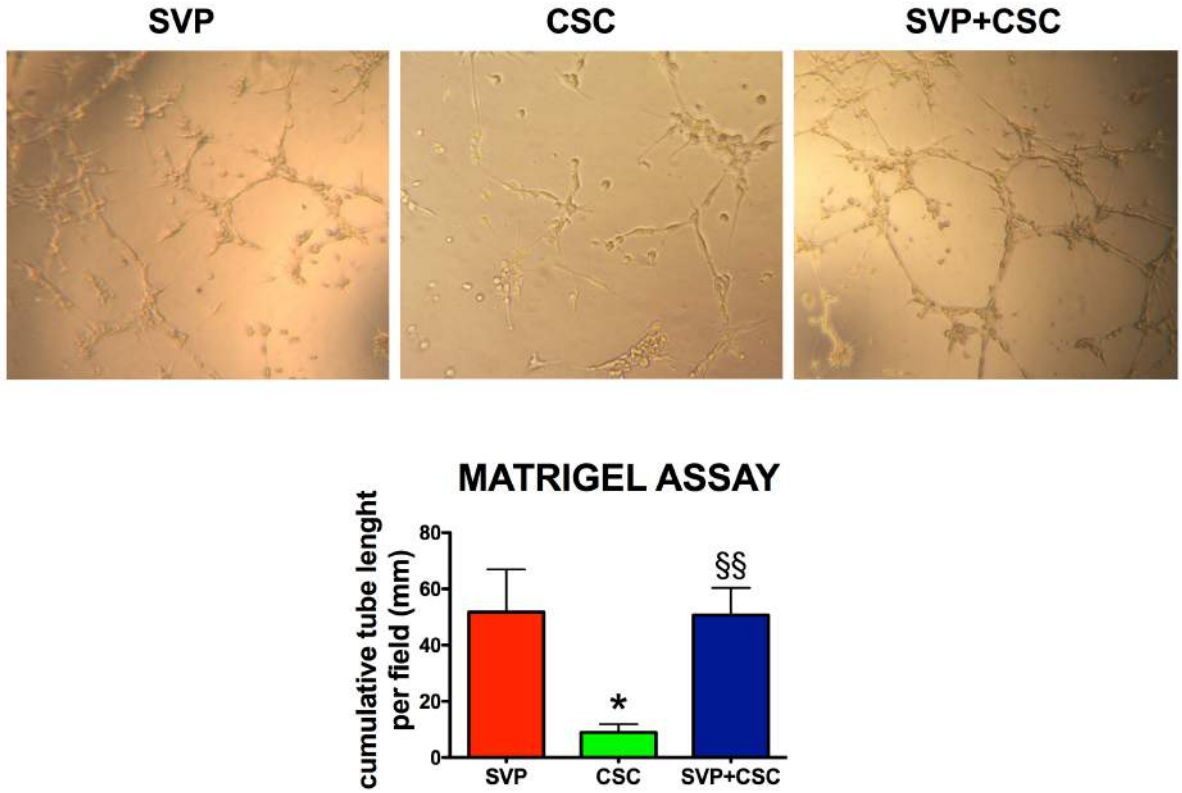

Online figure IX. In vitro **matrigel assay with SVPs, CSCs and SVPs+CSCs.** Representative phase-contrast optical images of SVPs, CSCs and SVPs+CSCs forming tubular networks when cultured for 5 hrs on Matrigel substrate. Magnification: 100X. Histograms summarize quantitative data of the tube length per field. Data are represented as mean±SEM. n=4 per each group. * $p<0.05$ vs. SVPs, §§ $p<0.01$ vs CSCs.

Circulation Research
JOURNAL OF THE AMERICAN HEART ASSOCIATION

Combined Intramyocardial Delivery of Human Pericytes and Cardiac Stem Cells Additively Improves the Healing of Mouse Infarcted Hearts Through Stimulation of Vascular and Muscular Repair

Elisa Avolio, Marco Meloni, Helen L. Spencer, Federica Riu, Rajesh Katare, Giuseppe Mangialardi, Atsuhiko Oikawa, Iker Rodriguez-Arabaolaza, Zexu Dang, Kathryn Mitchell, Carlotta Reni, Valeria V. Alvino, Jonathan Rowlinson, Ugolini Livi, Daniela Cesselli, Gianni Angelini, Costanza Emanueli, Antonio P. Beltrami and Paolo Madeddu

Circ Res. 2015;116:e81-e94; originally published online March 23, 2015;
doi: 10.1161/CIRCRESAHA.115.306146
Circulation Research is published by the American Heart Association, 7272 Greenville Avenue, Dallas, TX 75231

Print ISSN: 0009-7330. Online ISSN: 1524-4571